

MICROBIOME

Microbial ecology perturbation in human IgA deficiency

Jehane Fadlallah,^{1*} Hela El Kafsi,^{1*} Delphine Sterlin,^{1,2} Catherine Juste,³ Christophe Parizot,² Karim Dorgham,¹ Gaëlle Autaa,¹ Doriane Gouas,¹ Mathieu Almeida,⁴ Patricia Lepage,³ Nicolas Pons,⁵ Emmanuelle Le Chatelier,⁵ Florence Levenez,⁵ Sean Kennedy,⁵ Nathalie Galleron,⁵ Jean-Paul Pais de Barros,^{6,7} Marion Malphettes,⁸ Lionel Galicier,⁸ David Boutboul,^{8,9} Alexis Mathian,¹⁰ Makoto Miyara,^{1,2} Eric Oksenhendler,^{8,11} Zahir Amoura,^{1,10} Joel Doré,^{3,5} Claire Fieschi,^{8,9} S. Dusko Ehrlich,^{5,12} Martin Larsen,^{1,2†‡} Guy Gorochov^{1,2†‡}

Copyright © 2018
The Authors, some
rights reserved;
exclusive licensee
American Association
for the Advancement
of Science. No claim
to original U.S.
Government Works

Paradoxically, loss of immunoglobulin A (IgA), one of the most abundant antibodies, does not irrevocably lead to severe infections in humans but rather is associated with relatively mild respiratory infections, atopy, and autoimmunity. IgA might therefore also play covert roles, not uniquely associated with control of pathogens. We show that human IgA deficiency is not associated with massive quantitative perturbations of gut microbial ecology. Metagenomic analysis highlights an expected pathobiont expansion but a less expected depletion in some typically beneficial symbionts. Gut colonization by species usually present in the oropharynx is also reminiscent of spatial microbiota disorganization. IgM only partially rescues IgA deficiency because not all typical IgA targets are efficiently bound by IgM in the intestinal lumen. Together, IgA appears to play a nonredundant role at the forefront of the immune/microbial interface, away from the intestinal barrier, ranging from pathobiont control and regulation of systemic inflammation to preservation of commensal diversity and community networks.

INTRODUCTION

Eukaryotes have developed spectacular ways not only to protect themselves from pathogens but also to benefit from unique and essential features of surrounding organisms (symbionts). Mammals are indeed highly dependent on their consortia of symbionts (microbiota) that serve both to optimize processing of nutrients and to protect from opportunistic agents by competition. Innate immune mechanisms controlling host-microbiota mutualism are physically localized, activated by bacterial contact, culminating into breach of the gut mucosal firewall. Immediate nonspecific host responses involve the secretion of defensins and the intraluminal recruitment of innate immune cells such as neutrophils that encapsulate commensals and limit their contact with surrounding gut epithelium (1). Such a potent response comes with a fitness cost to the commensal community and the benefits this brings to the host. It is therefore postulated that an evolutionary pressure took place to acquire mechanisms acting in the lumen, which would regulate microbial communities, thereby reducing the frequency of breaching

the gut barrier and activation of innate immunity. This role could be played by antibodies and, most likely, by secretory immunoglobulin A (IgA) (2, 3). However, whereas antibody responses to pathogens have been intensively studied, much less interest has been devoted to the study of antibody relations with symbionts. Murine models of IgA deficiency (IgAd) have been studied and display modifications of the microbiome-immune interface. In such models, IgAd was obtained by inducing (i) defects in IgA class switch recombination (CSR) (4–6), (ii) defects in IgA transport into the gut lumen [pIgR^{-/-} mice (7, 8) and J-chain^{-/-} mice (9)], or (iii) reduction of IgA repertoire diversity without altering IgA levels [(activation-induced cytidine deaminase knock-in mutation (10), PD-1^{-/-} mice (11), and FoxP3⁺CD4⁺-depleted mice (12)]. Models impairing CSR mechanisms (i) are associated with a gut dysbiosis defined by an expansion of anaerobes, predominantly segmented filamentous bacteria (SFB) and *Clostridiales*, as well as nodular hyperplasia secondary to hyperactivation of germinal center B cells induced by microbial antigens (4, 5). Models impairing IgA secretion (ii) into the gut lumen were associated with altered microbiota composition, increased susceptibility to induced colitis, higher bacterial translocation to mesenteric lymph nodes after *Salmonella typhimurium* challenge, and lack of protective immunity against cholera toxin (7, 8). Notably, alterations of gut microbiota ecosystems were observed in the small intestine, whereas large intestine communities were much less affected by the absence of IgA (5), possibly because IgA predominantly targets commensal bacteria in the small intestine, but not in the colon, as shown by Bunker *et al.* (13) both in mice and in humans. Together, altered microbiome composition, increased susceptibility to microbial translocation, reduced microbial diversity, and reduced microbial fitness are shared features of IgA deficiency models.

These results are in line with the initial conception of IgA function, mainly presented as a neutralizing antibody, whose role would mainly be to exclude potentially harmful microbes and toxins from intimate contact with intestinal epithelia, thereby preserving mucosal barrier integrity (14). IgAd is relatively common in human adults, occurring in about 1 in 500 Caucasian individuals (15, 16). Although

¹Sorbonne Université, INSERM, Centre d'Immunologie et des Maladies Infectieuses-Paris (CIMI-Paris), 75013 Paris, France. ²Assistance Publique-Hôpitaux de Paris (AP-HP), Groupement Hospitalier Pitié-Salpêtrière, Département d'Immunologie, 75013 Paris, France. ³UMR1319 Micalis, Institut National de la Recherche Agronomique (INRA), Jouy-en-Josas, France. ⁴Center for Bioinformatics and Computational Biology, University of Maryland, Paint Branch Road, College Park, MD 20742, USA. ⁵INRA, US1367 MetaGenoPolis, 78350 Jouy en Josas, France. ⁶INSERM, LNC UMR866, University Bourgogne Franche-Comté, F-21000 Dijon, France. ⁷LIPoprotéines et Santé prévention & Traitement des maladies Inflammatoires et du Cancer (LipSTIC) LabEx, Fondation de Coopération Scientifique Bourgogne-Franche Comté, F-21000 Dijon, France. ⁸Département d'Immunologie Clinique, Hôpital Saint-Louis, AP-HP, 75010 Paris, France. ⁹INSERM U1126, Université Paris Diderot Paris 7, 75010 Paris, France. ¹⁰Assistance Publique-Hôpitaux de Paris (AP-HP), Groupement Hospitalier Pitié-Salpêtrière, Service de Médecine Interne 2, Institut E3M, 75013 Paris, France. ¹¹Université Paris Diderot Paris 7, EA3518, 75010 Paris, France. ¹²King's College London, Centre for Host-Microbiome Interactions, Dental Institute Central Office, Guy's Hospital, London, UK.

*These authors contributed equally to this work.

†These authors jointly directed this work.

‡Corresponding author. Email: martin.larsen@upmc.fr (M.L.); guy.gorochov@upmc.fr (G.G.)

human selective IgA deficiency (SIgAd) (that is, patients deficient for IgA but sufficient for all other antibody isotype) was, for a long time, considered asymptomatic, recent longitudinal studies have revealed that 80% of patients are symptomatic, when assessing complications more broadly (17) or when follow-up is extended (18). Human IgAd is associated with recurrent mucosal infections, autoimmunity, and intestinal disorders such as inflammatory bowel disease (IBD) and lymphoid hyperplasia (19, 20). To explain the mild phenotype observed in SIgAd patients, it is proposed that IgM may effectively replace IgA as the predominant antibody in secretions (21, 22). However, if IgA indeed represents a merely redundant component of the immune system, then it appears paradoxical that it was so well conserved in evolution and that it is massively produced at the individual level [about 66 mg/kg per day of IgA is secreted everyday (23)]. IgA also appears to orchestrate the beneficial tolerance established between the host and its gut commensal microbiome. These mutualistic host-microbial relationships were emphasized in animal models with an immune system reduced to a single monoclonal antibody of known bacterial specificity challenged by a limited microbial diversity. Although antibody binding was reducing bacterial fitness, it also resulted in reduced intestinal production of proinflammatory signals, hence allowing bacterial tolerance by the host (24). Similarly, flagellin-specific secretory IgA (sIgA) may promote tolerance by reducing bacterial motility through modulation of flagellin transcription (25).

Although these models have provided important examples and possible mechanisms through which antibodies can imprint specific microbes, the targets of polyclonal IgA and their global impact on the microbiome remain poorly defined. Although it was recently shown in an animal model that IgA-coated bacteria include proinflammatory elements (26), it is not known whether IgA preferentially binds potentially harmful bacteria and/or commensals (27). It is not known either whether IgM can indeed replace IgA at no expense to host/bacterial homeostasis. Finally, the relations between SIgAd and systemic autoimmunity are not well understood.

Here, we studied the composition of sIgA-bound gut microbiota in healthy individuals and evaluated alterations of this bacterial consortium in SIgAd patients. To get insights into the specific contributions of IgA on host/microbial symbiosis, we also explored systemic immune responses in these patients.

RESULTS

Patients lacking IgA-producing B cells and seric IgA also lack free and bacteria-bound digestive IgA

SIgAd represents a bioclinical entity that is defined by serologic means, namely, undetectable seric IgA titers (<0.07 mg/ml) with normal IgG concentration (28). SIgAd patients are known to present low or undetectable salivary IgA levels (21, 22), but their gut IgA status had not been assessed. We serologically confirmed a status of IgA deficiency in 21 patients that could be included in this study because, among other exclusion criteria, they did not receive antibiotic treatment 3 months before inclusion. Compared to age- and sex-matched healthy donors (HDs) ($n = 34$), these SIgAd patients had undetectable seric (fig. S1A) and scarce digestive IgA levels [43 (0 to 206) μ g in HDs versus 0 (0 to 21) μ g of free IgA per gram of stool in SIgAd, $P < 0.0001$; Fig. 1A], whereas their seric IgG levels were preserved (fig. S1B).

Circulating IgA⁺ B cells were undetectable in all patients except one [0.1 (0 to 1.3)% in SIgAd versus 7.1 (2.4 to 14.4)% in HDs, $P < 0.0001$], whereas proportion of CD19⁺IgG⁺ cells among B cells was

similar in both groups [12.55 (5.32 to 29.6)% versus 13.1 (0.793 to 37.6)%, $P = 0.8004$; Fig. 1B]. Compared to controls, SIgAd patients are also characterized by a depletion of CD19⁺CD27⁺IgD⁻ switched memory B cells among total CD19⁺ B cells [20 (5.17 to 34.1)% versus 14.9 (3.3 to 38.1)%, $P = 0.0328$; Fig. 1C]. These data show that sIgA deficiency affects both peripheral blood and distant organs, such as the intestine, at both the cellular and the protein level.

The clinical spectrum of digestive SIgAd-associated symptoms varies from very mild to severe, and it remains unknown whether residual digestive IgA would account for pauci-symptomatic presentations. We therefore used a flow cytometry assay, derived from our previously published technology (29), to test whether traces of IgA might be detected at the surface of the fecal microbiota, although free digestive IgA is usually not detectable in SIgAd, as shown above. The protocol was modified to assess levels of mucosal antibodies targeting colonic microbiota in vivo (Fig. 1D). IgA, as the main mucosal antibody in HDs, binds a median percentage of 7.6 (0.8 to 17.6)% of the whole fecal microbiota (Fig. 1D). Close examination of flow cytometry profiles also reveals that IgA-bound microbiota can be subdivided into IgA^{dim} and IgA^{bright} bacterial populations (Fig. 1D, left). These IgA⁺ subsets were absent in all SIgAd patients except one ($P < 0.0001$; Fig. 1D, right). Notably, this patient also had detectable IgA⁺ circulating B cells (Fig. 1B). This interesting case confirms that some patients diagnosed with SIgAd by serologic means indeed retain sIgA, which can be detected by the very sensitive bacterial flow cytometry technique. These data nevertheless establish that microbiota-bound IgA is usually undetectable in SIgAd patients.

Global microbiome diversity is preserved in SIgAd patients

To study the global impact of digestive IgA deficiency on the gut microbiome, we performed shotgun sequencing (30, 31) of fecal samples in 34 HDs and 17 SIgAd patients. High-quality reads from each sample were mapped to a reference catalog of 3.9 million genes (32). Taxonomic abundances were computed at the level of co-abundance gene groups (CAGs) and, subsequently, binned at broader taxonomic levels (genus, family, order, class, and phylum). CAGs contain at least 50 different genes. Metagenomic species (MGSs) are defined as larger CAGs with very high connectivity and a defined minimal size of at least 700 genes. This approach to study microbiome composition presents the advantage to overcome the limited resolution of previous methods used for metagenomic or 16S amplicon data analysis that rely on comparisons to reference genomes, offering the possibility to comprehensively profile the diversity of a clinical sample and to potentially identify previously uncharacterized microbes (32).

Metagenomic analysis revealed a similar representation of the dominant phyla in the two groups [HDs versus SIgAd: 44.55% versus 45.52% ($P = 1$) for Bacteroidetes, 50.52% versus 48.35% ($P = 0.7774$) for Firmicutes, 2.19% versus 3% ($P = 1$) for Proteobacteria, 0.65% versus 0.84% ($P = 0.99$) for Actinobacteria, and 1.5% versus 1.41% ($P = 1$) for unclassified phyla; fig. S2A]. Microbiota diversity was not different between the two groups, either when including all MGS regardless of their phylum [median Shannon index, HDs versus SIgAd: 4.008 (2.501 to 4.698) versus 3.946 (1.690 to 4.511), $P = 0.6344$] or when comparing MGS diversity within each phylum [HDs versus SIgAd: 2.529 (1.225 to 3.380) versus 2.564 (0.8064 to 3.234), $P = 0.8180$ for Bacteroidetes; 3.978 (3.067 to 4.619) versus 3.779 (2.735 to 4.286), $P = 0.05$ for Firmicutes; 1.688 (1.170 to 2.223) versus 1.699 (0.5898 to 2.131), $P = 0.8421$ for Actinobacteria; 1.432 (0.1518 to 2.132) versus

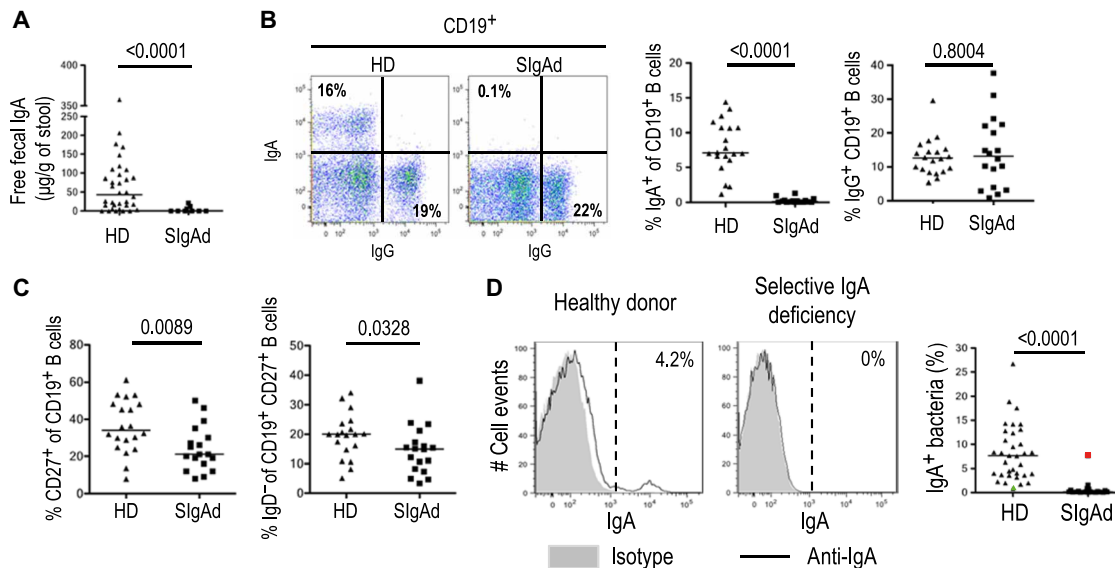


Fig. 1. Immunological phenotype of stool and blood from SIgAd patients. (A) Free IgA levels in fecal water were measured by enzyme-linked immunosorbent assay (ELISA) in HDs ($n = 34$) and SIgAd patients ($n = 21$). (B) $CD19^+IgA^+$ and $CD19^+IgG^+$ cells (C) peripheral $CD19^+CD27^+$ (memory B cells) and $CD19^+CD27^+IgD^-$ (switched memory B cells) cells were detected by flow cytometry surface staining. (D) SIgA-binding levels of ex vivo purified and fixed microbiota are measured by a flow cytometry-based assay. Gray histograms represent isotype control, and black lines represent anti-IgA-stained microbiota. In the graphs, each symbol represents a donor (34 HDs and 21 SIgAd). In all sections, horizontal bars represent medians. Indicated P values were calculated using a Mann-Whitney test. An HD with nondetectable IgA binding of gut microbiota and an SIgAd patient with detectable IgA binding of gut microbiota are indicated with a green and red symbol, respectively.

1.432 (0.3349 to 2.014), $P = 0.9042$ for Proteobacteria; and 2.283 (0.6089 to 2.830) versus 2.032 (1.161 to 2.687), $P = 0.1357$ for unclassified phyla; fig. S2B]. Furthermore, no significant difference was observed in terms of median MGS richness between the two groups [454 (215 to 694) different MGS detected in HDs versus 451 (160 to 641) in patients, $P = 0.7553$; fig. S2C] nor in gene count [395841 (236166 to 636394) genes in HDs versus 379482 (248232 to 514298) genes in patients, $P = 0.4167$; fig. S2C]. To estimate the stability of the gut microbiota profiles, we analyzed the gut microbiota composition of three healthy subjects sampled longitudinally (two samples, 12 months apart). Hierarchical cluster analysis outlines strong structural intra-individual sample proximity, suggesting overall temporal stability of individual gut microbiota profiles, at least in healthy subjects (fig. S3). Together, these data reveal that the diversity of SIgAd and control fecal bacterial repertoires does not differ significantly. Our data also suggest that an individual's profile remains stable over time.

IgA deficiency gut microbiota displays mild dysbiosis

We reasoned that IgA deficiency might affect relatively discrete bacterial populations, without affecting global microbiome structure at the analysis level applied above. A gene biomarker approach (33) was used to determine which bacteria were expanded or depleted in IgA deficiency, comparing the whole unsorted microbiota of 34 HDs with 17 SIgAd patients (fig. S4). We found 31 differential MGSs between the two groups; 17 being overrepresented, whereas 14 were underrepresented in SIgAd patients. Differential MGSs, between controls and patients, were ranked according to increasing statistical significance (Fig. 2A). Most MGSs depleted in IgA deficiency (13 of 14) belong to the Firmicutes phylum, whereas only one belongs to the Bacteroidetes phylum. Among depleted Firmicutes, more than half of them (7 of 13) belong to the *Lachnospiraceae* family, and two are *Ruminococcaceae* (*Faecalibacterium* genus, $n = 2$ of 2) (Fig. 2B).

Conversely, among the 17 expanded MGSs in IgA deficiency, 10 are Firmicutes, 4 are Bacteroidetes, and 3 are Proteobacteria (Gamma-proteobacteria exclusively, including *Escherichia coli*). These 17 MGSs belong to 11 different families and, thus, are more diverse than depleted species. Three of seventeen expanded MGSs are usually present in the oropharynx flora (*Streptococcus sanguinis*, *Veillonella parvula*, and *Haemophilus parainfluenzae*). In addition, we found two different species of *Prevotella* to be overrepresented in SIgAd (compare Fig. 2A).

IgA targets more likely decline than expand in the absence of IgA

We then postulated that microbial ecology perturbation in the absence of IgA might be appreciated in a different manner if we could focus on bacteria, more specifically, IgA-targeted in healthy controls. We previously verified that metagenomic analysis could reliably be performed on sorted bacterial subsets with a determined lowest analyzable sample size of 10^8 bacteria (34). IgA^+ fractions were enriched by magnetic sorting in 30 healthy controls, allowing IgA^+ and IgA^- fraction sequencing and differential metagenomic analysis (Fig. 3A). The same gene biomarker identification approach as above (fig. S4) allowed the identification of 24 different MGS overrepresented in the IgA^+ fraction of healthy controls (fig. S5). These " IgA^+ MGSs" were ranked according to increasing statistical significance at the lowest taxonomic level available (Fig. 3B). Among the 24 IgA^+ MGSs, 19 belong to the Firmicutes phylum (among which 12 belong to the Clostridia class, 1 of these 12 belonging to the *Faecalibacterium* genus), 2 are bacteria from unclassified phylum, 1 is Proteobacteria (one *E. coli* species), 1 belongs to the Actinobacteria phylum (*Bifidobacterium bifidum*), and the last identified MGS belong to the Bacteroidetes phylum (Fig. 3C). We finally compared the prevalence of IgA^+ MGSs between SIgAd patients and controls and found that the prevalence of only four of them was significantly altered (Fig. 3D). Whereas *E. coli* (CAG 4) was

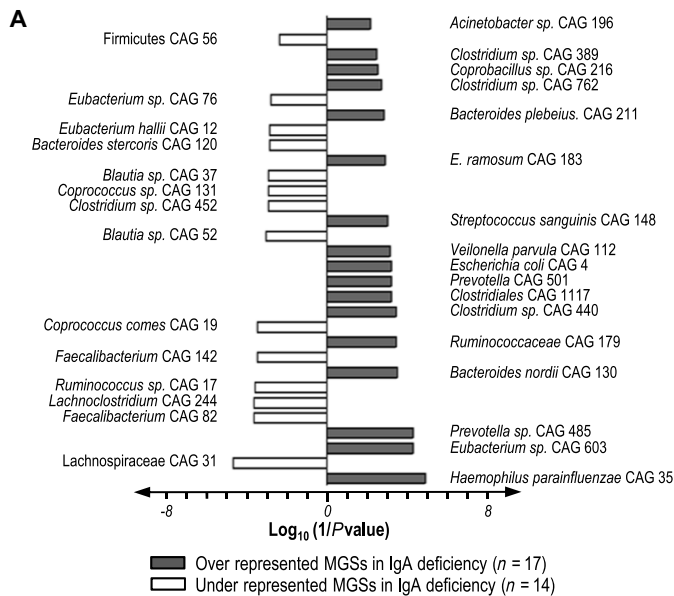
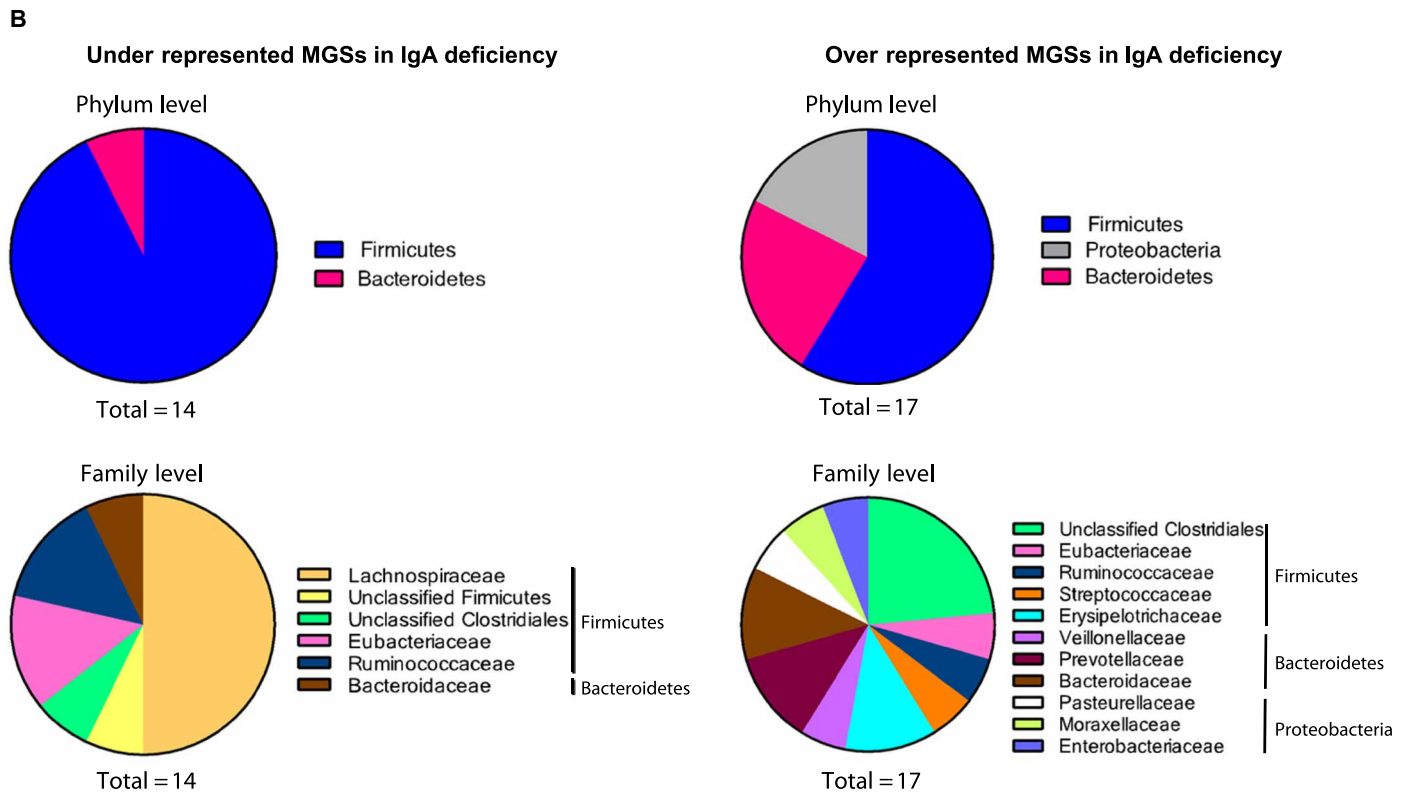


Fig. 2. Bacterial repertoire shift associated with IgA deficiency. (A) Differential MGS ($n = 31$) between SIgAd patients and HDs assigned at their lowest taxonomic level and ranked by statistical difference. White histograms represent MGSs that are underrepresented in IgA deficiency ($n = 14$), whereas gray histograms represent MGSs that are overrepresented in IgA deficiency ($n = 17$), compared to HDs. (B) Taxonomic distribution at phylum (top row) and family (bottom row) level of underrepresented MGS (left column) and overrepresented MGS in IgA deficiency.



found to be expanded in patients, we rather observed that *Coprococcus comes* (CAG 19), *Clostridium* sp. (CAG 138), and *Dorea* sp. (CAG 73) were depleted in SIgAd (Fig. 3E). Together, the prevalence of most IgA⁺ MGSs does not vary significantly in SIgAd. Furthermore, an IgA⁺ MGS does not systematically expand in the context of SIgAd.

IgM digestive secretion partially rescues microbiota antibody coating in SIgAd patients

We then postulated that compensatory immune mechanisms might explain why IgA deficiency is not associated with massive perturba-

tions of gut microbial ecology, as previously suggested (21, 22, 35). Microbial flow cytometry analysis was used to detect other antibody isotypes on the surface of SIgAd microbiomes. IgM was indeed detected at the surface of SIgAd microbiota in all SIgAd patients analyzed (Fig. 4A). IgM bound 6.26 (0.625 to 45)% ($n = 21$) of the whole microbiome in patients, whereas IgM binding was observed in minimal amounts in only 2 of 34 healthy controls [0.05 (0 to 2.4)%, $P < 0.0001$; Fig. 4B]. Measured free fecal IgM levels were consistent with IgM-bound levels [0.83 (0 to 28.1) μ g and 39.9 (0 to 436.1) μ g of free IgA per gram of feces in HDs and SIgAd patients, respectively, $P = 0.0004$; Fig. 4B].

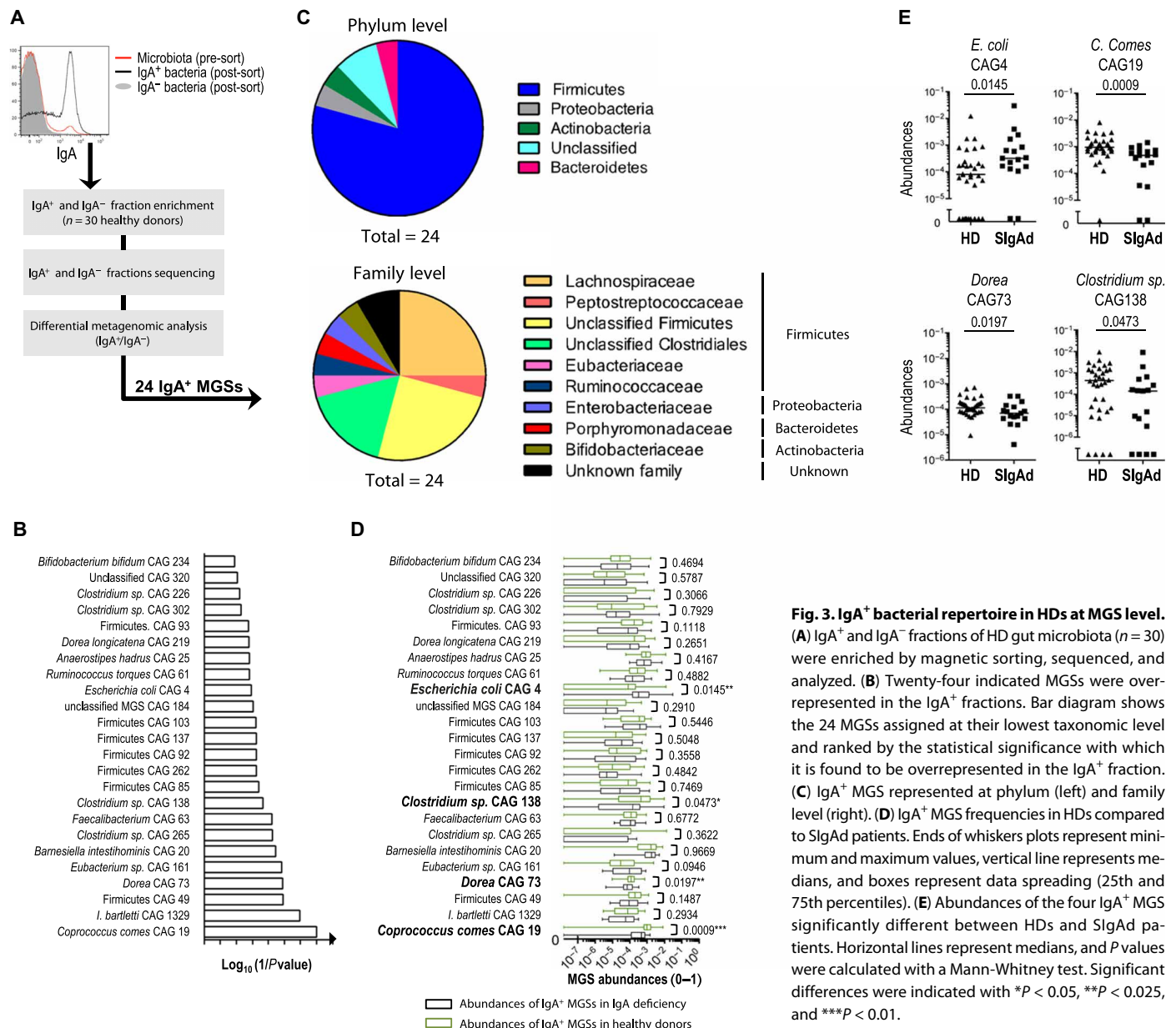


Fig. 3. IgA⁺ bacterial repertoire in HDs at MGS level. (A) IgA⁺ and IgA⁻ fractions of HD gut microbiota (n = 30) were enriched by magnetic sorting, sequenced, and analyzed. (B) Twenty-four indicated MGSs were over-represented in the IgA⁺ fractions. Bar diagram shows the 24 MGSs assigned at their lowest taxonomic level and ranked by the statistical significance with which it is found to be overrepresented in the IgA⁺ fraction. (C) IgA⁺ MGS represented at phylum (left) and family level (right). (D) IgA⁺ MGS frequencies in HDs compared to SIgAd patients. Ends of whiskers plots represent minimum and maximum values, vertical line represents medians, and boxes represent data spreading (25th and 75th percentiles). (E) Abundances of the four IgA⁺ MGS significantly different between HDs and SIgAd patients. Horizontal lines represent medians, and P values were calculated with a Mann-Whitney test. Significant differences were indicated with *P < 0.05, **P < 0.025, and ***P < 0.01.

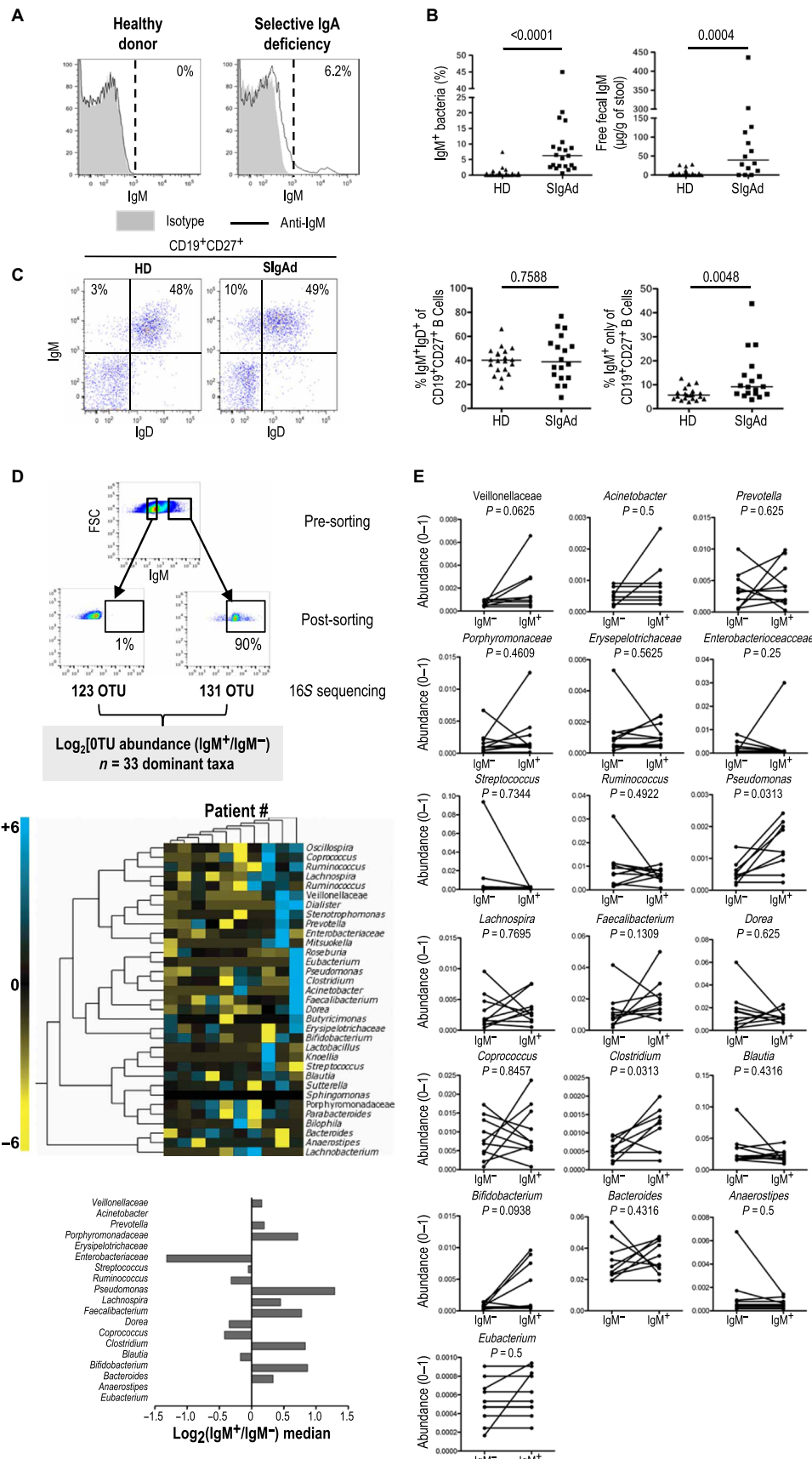
In blood, so-called IgM-only B cells (36) (CD19⁺CD27⁺IgM⁺IgD⁻) were increased in patients [5.67 (2.88 to 12.73)% in HDs versus 9.14 (3.83 to 43.75)% in SIgAd patients, P = 0.0048], whereas marginal zone-like cells (CD19⁺CD27⁺IgM⁺IgD⁺) are similar in both groups [40.2 (17.8 to 66.3)% and 38.85 (9.29 to 76.8)% in HDs and SIgAd patients, respectively, P = 0.7588; Fig. 4C]. Therefore, in the absence of IgA, IgM is secreted to the digestive tract, where it binds gut commensals. Our data also suggest that CD19⁺CD27⁺IgM⁺IgD⁻ B cell expansion could account for this compensatory measure.

We then asked whether IgM could be looked upon as a surrogate for IgA at the immune-microbiota interface. To test whether IgM and IgA bind overlapping repertoires of bacteria, we separated IgM⁺ and IgM⁻ bacteria from patient's microbiomes (n = 10) using flow cytometry. Metagenomic analysis could not be performed on sorted samples because the lowest analyzable sample size of 10⁸ bacteria was not reached for all IgM⁺ fractions. Bacterial fractions were then

identified by 16S rRNA sequencing (Fig. 4D, top). Hierarchical clustering of n = 33 dominant taxa abundance ratios [$\log_2(\text{IgM}^+/\text{IgM}^-)$] displays no evidence of a common pattern of IgM recognition (Fig. 4D, middle). Thus, much like IgA responses (fig. S6), IgM responses also seem to be highly variable interindividually.

We then focused our analysis on the taxa bound by SIgA, or differing between HDs and SIgAd patients, (confer Figs. 3B and 2A, respectively). Using the median $\log_2(\text{IgM}^+/\text{IgM}^-)$ ratios of all the donors, we found that (i) Veillonellaceae family, *Prevotella* genus, Porphyromonadaceae family, *Pseudomonas* genus, *Lachnospira* genus, *Faecalibacterium* genus, *Clostridium* genus, *Bifidobacterium* genus, and *Bacteroides* genus are overrepresented in IgM⁺ fraction; (ii) *Enterobacteriaceae* family, *Streptococcus* genus, *Ruminococcus* genus, *Dorea* genus, *Coprococcus* genus, and *Blautia* genus are overrepresented in IgM⁻ fraction; and (iii) *Acinetobacter* genus, *Erysipelotrichaceae* family, *Anaerostipes* genus, *Eubacterium* genus

Fig. 4. IgM binding to SigAd microbiota. (A) Representative flow cytometry–based IgM detection on purified microbiota in an HD and an SigAd patient. Gray histograms represent isotype controls, and black lines represent IgM surface staining. (B) IgM binding in HDs ($n = 34$) and SigAd patients ($n = 21$) measured by flow cytometry (left). Free IgM levels in fecal waters measured by ELISA (right). (C) Peripheral $CD19^+CD27^+IgM^+IgD^+$ (circulating marginal zone B cells) and $CD19^+CD27^+IgM^+IgD^-$ (“IgM only” B cells) frequencies in HDs and patients. (D) IgM^+ and IgM^- fractions of gut microbiota were sorted by flow cytometry in 10 patients, and their composition was analyzed by 16S ribosomal RNA (rRNA) gene sequencing (top). Taxa enrichment in IgM^+ fraction is measured as the $\log_2(IgM^+/IgM^-)$ ratio of OTU abundances. The taxa enrichment measures of 33 dominant OTUs (rows) were grouped by hierarchical cluster analysis according to Ward’s method and plotted as a heat map. Each column represents a patient. Yellow and cyan colors represent the lowest and highest ratios, respectively (range of the ratios: -6 to $+6$, middle). Medians of the IgM^+ enrichment ratio. Each horizontal bar represents the median ratio of the 10 donors by OTU (bottom). (E) Paired analysis of the abundances in IgM^+ and IgM^- fractions for each OTU of interest. In (B) and (C), horizontal bars represent medians, and Mann-Whitney test was used to calculate P values. In (E), P values were calculated with a paired-rank Wilcoxon test. FSC, forward scatter.



are equally present in both fractions (Fig. 4D, bottom). Paired analysis performed on these 19 taxa revealed that *Clostridium* and *Pseudomonas* genera are significantly enriched in the IgM⁺ fraction ($P = 0.013$). Bacteria belonging to the *Enterobacteriaceae* family are poorly bound by IgM. Together, not all typical IgA targets are bound by digestive IgMs in SIgAd patients (Fig. 4E).

IgM responses are correlated with commensal diversity in IgA deficiency

Given that the recent literature substantiates that IgA shapes microbiota composition and diversity in mice (12), we wanted to know whether

IgM could play this role in IgA deficiency. Median gut IgM⁺ enrichment ratios based on operational taxonomic unit (OTU) abundances calculated at phylum level in IgM⁺- and IgM⁻-sorted fractions were correlated with the Shannon diversity index (fig. S2B) within each dominant phylum in nine SIgAd patients (Fig. 5A). As shown, IgM⁺ enrichment ratio is positively correlated with Actinobacteria phylum diversity (Spearman coefficient, $r = 0.7167$; $P = 0.0369$), whereas no statistical correlation is observed for the three other dominant phyla. Notably, the very narrow range of IgM binding to Firmicutes, and to some extent Proteobacteria, might have precluded identification of potential correlations between IgM binding and diversity in these phyla.

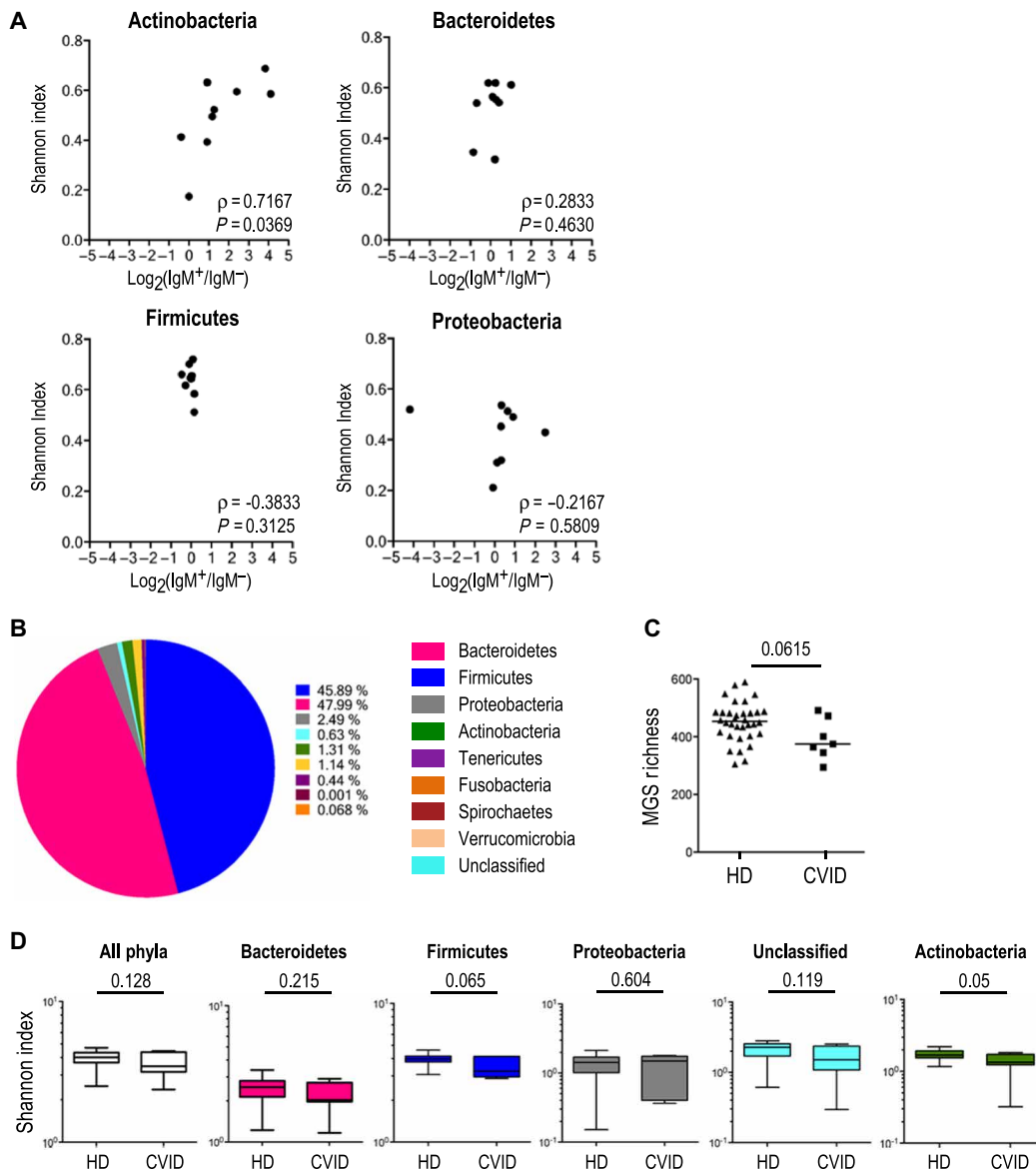


Fig. 5. IgM binding and microbial diversity. (A) Scatter graphs represent the correlation between phylum enrichment in the IgM⁺ fraction [$\log_2[(\text{IgM}^+)/(\text{IgM}^-)]$], where (IgM⁺) and (IgM⁻) represent phylum abundances in the IgM⁺ and IgM⁻ fractions, respectively) and microbial diversity within each of the top four most dominant phyla (Shannon diversity index) calculated from metagenomic sequencing (confer Fig.1) in $n = 9$ patients with SIgAd. Spearman coefficient (ρ) and P values (P) are indicated. (B) Phyla distribution, (C) MGS richness, and (D) diversity are shown for $n = 7$ patients with common variable immunodeficiency (CVID). Diversity is calculated with Shannon's diversity index either for all the MGS (white whiskers plot) or within each phylum. Ends of whiskers represent the minimum and maximum of all the data, and boxes represent data spreading (1 SD). Horizontal bars represent medians, and P values were calculated with a Mann-Whitney test.

Serum IgM responses against two strains belonging to the Actinobacteria phylum (*Bifidobacterium adolescentis* and *Bifidobacterium longum*) were confirmed in 16 HDs by flow cytometry (fig. S7A). We then postulated that Actinobacteria diversity could be further reduced in the absence of IgM. We therefore explored CVID patients with total IgA deficiency and very low or undetectable IgM digestive levels [0 (0 to 115) μg of free IgM per gram of stool; fig. S7B]. As expected, IgM gut microbiota binding is minimal [0.297 (0.08 to 3.84)%, $n = 15$; fig. S7C] in CVID. Shotgun sequencing of the whole CVID gut microbiota and metagenomic analysis (Fig. 5B) suggested a significant global loss of MGS richness [454 (305 to 590) in HDs ($n = 34$) versus 375 (294 to 491) in CVID ($n = 7$), $P = 0.0615$; Fig. 5C]. A significant loss in Actinobacteria phylum diversity was observed in these patients [Shannon diversity index, 1.688 (1.170 to 2.223) in HDs versus 1.342 (0.319 to 1.827) in CVID; $P = 0.05$]. A loss, yet more moderate, of the Firmicutes phylum diversity was also observed ($P = 0.065$; Fig. 5D). Together, the data suggest that, in the absence of intestinal IgA, IgM binding preserves Actinobacteria diversity, although this conclusion needs to be validated on a larger CVID cohort.

IgA deficiency is associated with systemic inflammation

We then asked whether the lack of sIgA could induce perturbations in host systemic inflammatory versus regulatory responses, in spite of the presence of mucosal IgM responses. Cytokine-secreting circulating CD4⁺ T cells were measured in both groups (Fig. 6A). Proportions of interferon- γ (IFN- γ)⁺CD4⁺ T cells were not different [14.6 (3.3 to 25.7)% in HDs versus 16.75 (2.28 to 47.8)% in SIgAd, $P = 0.3932$], whereas interleukin-17 (IL-17)⁺CD4⁺ and IL-22⁺CD4⁺ T cells were increased in IgA deficiency [0.422 (0.04 to 1.96)% versus 0.866(0.02 to 4)%], $P = 0.0137$ and 0.136 (0.06 to 0.769)% versus 0.866(0.02 to 4)%, $P = 0.0104$, respectively]. Double-positive IL-17⁺IL-22⁺ CD4⁺ T cells were also increased in IgA deficiency [0.05 (0.02 to 0.44)% versus 0.2 (0 to 0.75)%, $P = 0.0058$]. Seric IL-6, IL-10, and IL-17 concentrations were all elevated in patients [0.6 (0.33 to 2.4) pg/ml versus 1 (0.25 to 34.37) pg/ml ($P = 0.0315$), 0.47 (0 to 1.41) pg/ml versus 0.87 (0.37 to 5.2) pg/ml ($P = 0.0001$), and 0.06 (0 to 1.47) pg/ml versus 0.21 (0.007 to 0.92) pg/ml ($P = 0.0215$), respectively; Fig. 6B]. sCD14 was increased in patient's sera [2063 (1147 to 4283) pg/ml versus 2841 (1399 to 5187) pg/ml, $P = 0.0023$; Fig. 6C], although LPS concentration was not significantly increased in the same samples [54.15 (23.40 to 77.92) versus 48.10 (34.57 to 97.33); Fig. 6C]. We also observed an increase in CD4⁺PD-1⁺ cells [7.11 (1.86 to 16.9)% versus 14 (3.13 to 31.6)%, $P = 0.0093$; Fig. 6C] in SIgAd patients. The circulating regulatory T cell (T_{reg}) compartment was not altered by IgA deficiency, because frequency of naive T_{regs} (CD45RA⁺FoxP3⁺ CD4⁺ T cells), effector T_{regs} (CD45RA⁻FoxP3^{bright} CD4⁺ T cells), and activated conventional T cells (CD4⁺CD45RA⁻FoxP3^{low}) was similar between patients and controls (Fig. 6D). Thus, SIgAd patients display a circulating skewed CD4⁺ T cell phenotype toward T helper 17 (T_H17) differentiation associated with an increase of seric sCD14, which is a marker of monocyte activation. Patients with malabsorption were excluded from the study because mucosal defects might grossly affect gut microbial ecology. We stratified patients in an effort to determine whether other clinical features such as infection, autoimmunity, or historic antibiotic treatments (at least 3 months before sampling) might be preferentially associated with inflammation. We found no correlations between clinical status and any of the elevated immunological markers mentioned above (Fig. 6, A to D). Together, the immunological and inflammatory modifications as-

sociated with SIgAd are not contributed by isolated patients presenting “extreme” clinical phenotypes.

IgA deficiency is associated with a disturbed bacterial dependency network

Bacterial symbiosis in the human gut notably implies that some bacteria depend on other bacteria for their persistence. Within such networks, and by definition, a dependent bacterium, called “satellite,” never occurs independently of another, coined “host,” in a given sample. Conversely, the same host may occur in a given sample independently of its satellites (Fig. 7A). This concept was initially promoted by Nielsen *et al.* (32), who identified a minimal obligatory network of 45 MGS-MGS dependency associations involving 60 MGSs (the same MGS can make several associations). To investigate the potential impact of IgA deficiency on bacterial dependency associations, we tested whether this minimal obligatory network was disturbed in IgA deficiency.

Main links defined by Nielsen *et al.* (32) were confirmed in HDs (90 to 100%), whereas the confirmed link percentage was more dispersed in SIgAd patients, ranging from 75 to 100% (Fig. 7B). On the basis of our HD MGS-MGS co-presence distribution, the 99% confidence interval was calculated according to a γ distribution defining a lower threshold of 84% of MGS-MGS co-presence, below which the population-level link was considered absent. In our HD cohort, 41 of 45 links were maintained at population level, whereas only 30 links were confirmed in SIgAd patients. The 11 links lost in SIgAd patients involved 21 MGS: 7 *Faecalibacterium* sp., 4 Firmicutes, 2 Clostridiales, 2 *Ruminococcus* sp., 2 *Prevotella*, 2 *Butyrivimonas virosa*, and 2 unknown MGSs (data file S1).

The resulting network of remaining bacterial dependencies for HDs and SIgAd patients is shown in Fig. 7C. In summary, IgA deficiency is associated with a disturbed bacterial dependency association network.

DISCUSSION

Similar to what was observed in murine models of IgAd (5), we found that IgA deficiency does not markedly alter global fecal microbiota composition in affected patients. However, our observations are limited to feces, and a more severe dysbiosis may be present in the small intestine, as shown in mouse models of IgA deficiency (5, 11–13). The combination of flow cytometry and metagenomic analysis proved useful to increase the resolution of the analysis on human fecal samples by monitoring alterations of commensals specifically bound by sIgA in healthy controls. More work will be necessary to determine whether IgA^{dim} and IgA^{bright} bacterial populations correspond to bacteria bound by high- versus low-affinity IgA, respectively, and whether these subsets have overlapping bacterial repertoires or not. Notably, IgA interactions with very low affinity are also suggested and could account for the very discrete, but global, bacterial flow cytometry profile shift consistently observed in HDs but not observed in SIgAd patients.

It could have been expected that commensals bound by sIgA in healthy subjects would all tend to expand in IgAd patients. In murine models of immune deficiency, IgA targets, such as *SFB* (26), expand in the absence of an effective IgA response (4, 12). We rather observed that MGSs defined in Fig. 3B as main IgA targets in controls do not systematically bloom in SIgAd patients. Most notably, *C. comes* (CAG 19) is underrepresented in SIgAd patients compared to controls. By contrast, another typical IgA target, such as *E. coli* (CAG 4), is overrepresented in SIgAd patients by an order of magnitude, compared

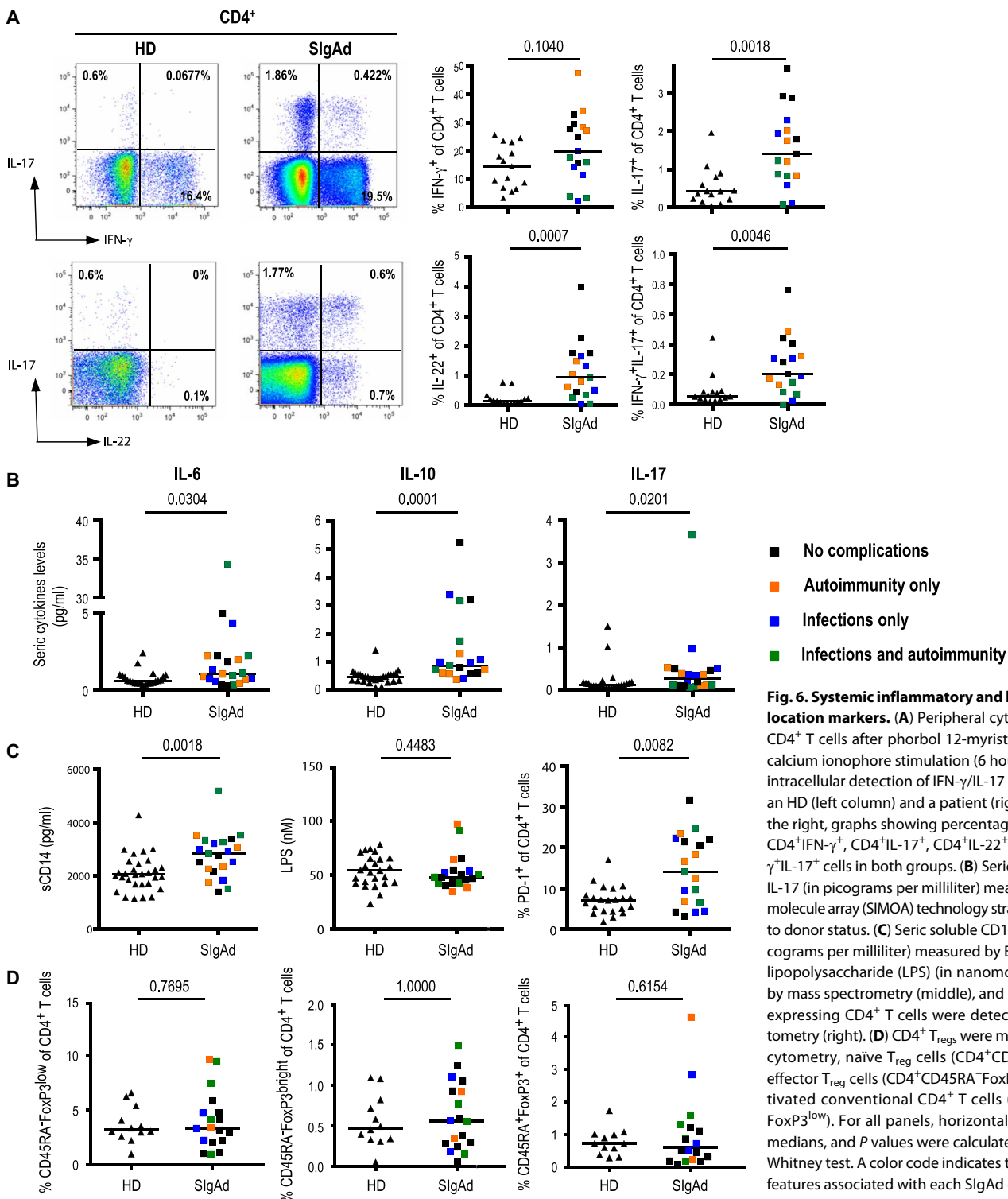


Fig. 6. Systemic inflammatory and bacterial translocation markers. (A) Peripheral cytokine-secreting CD4⁺ T cells after phorbol 12-myristate 13-acetate-calcium ionophore stimulation (6 hours). On the left, intracellular detection of IFN- γ /IL-17 or IL-17/IL-22 in an HD (left column) and a patient (right column). On the right, graphs showing percentages of peripheral CD4⁺IFN- γ ⁺, CD4⁺IL-17⁺, CD4⁺IL-22⁺, and CD4⁺IFN- γ ⁺IL-17⁺ cells in both groups. (B) Seric IL-6, and IL-17 (in picograms per milliliter) measured by single molecule array (SIMOA) technology stratified according to donor status. (C) Seric soluble CD14 (sCD14) (in picograms per milliliter) measured by ELISA (left), seric lipopolysaccharide (LPS) (in nanomolars) measured by mass spectrometry (middle), and peripheral PD-1 expressing CD4⁺ T cells were detected by flow cytometry (right). (D) CD4⁺ T_{regs} were measured by flow cytometry, naive T_{reg} cells (CD4⁺CD45RA⁺FoxP3⁺), effector T_{reg} cells (CD4⁺CD45RA⁻FoxP3^{bright}), and activated conventional CD4⁺ T cells (CD4⁺CD45RA⁻FoxP3^{low}). For all panels, horizontal bars represent medians, and P values were calculated with a Mann-Whitney test. A color code indicates the main clinical features associated with each SlgAd case.

to controls. These data suggest that *E. coli* (CAG4) expansion in the microbiota could indeed be negatively influenced by sIgA, whereas *C. comes* thrives in the presence of sIgA. More generally, at the family level, we observe that IgA⁺ bacteria are more likely found to be underrepresented than overrepresented in SlgAd patients. These data emphasize the

protective role that sIgA directly (or indirectly) plays in humans on commensal ecology, as previously observed in animal models (12).

Using the gene biomarker analytical approach described in Qin *et al.* (33), we identified bacterial targets of sIgA in HDs by metagenomic analysis of microbiota preparations enriched for sIgA-bound commensals.

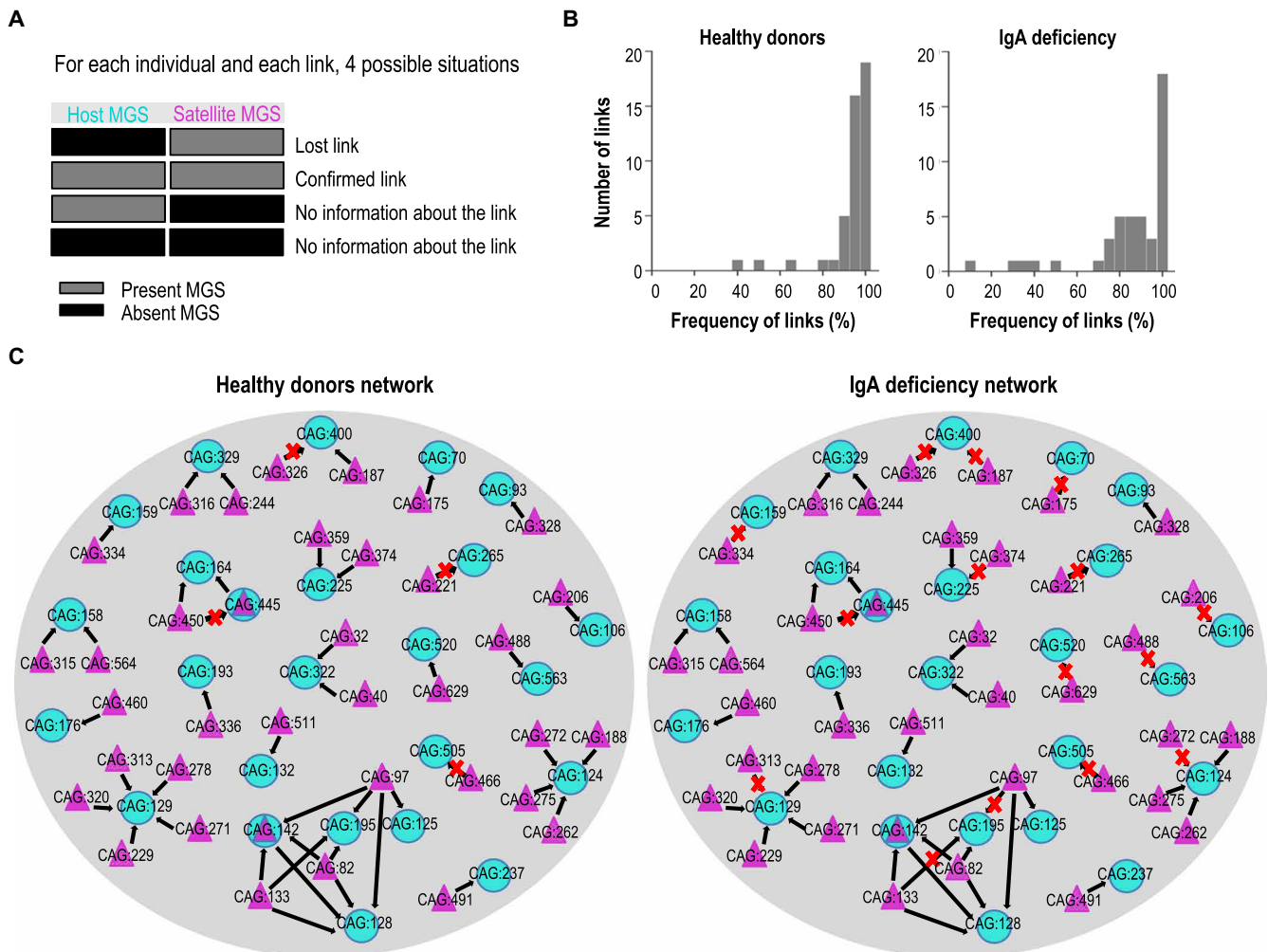


Fig. 7. Bacterial dependency networks in IgA deficiency and HDs. (A) For each individual and each MGS-MGS dependency, there are four possible situations. If the satellite MGS is present without corresponding host MGS, then the link is considered lost. If the satellite and host are both present, then the link is considered conserved. If the host is present in the absence of the satellite, or if both host and satellite are absent, then no information is given about the link. (B) Distribution of the percentage of confirmed MGS-MGS dependency links. (C) MGS-MGS dependency network compared between HDs (left) and SIgAd patients (right). Each of the two network maps shows the expected 45 highly significant and directional dependencies among 60 MGSs, as defined by Nielsen *et al.* (32). Blue circles represent host MGSs. Purple triangles represent satellite MGSs. A purple triangle within a blue circle indicates both satellite and host status. Black arrows indicate the confirmed dependencies among MGSs (directional arrow from the satellite MGS to the host MGS). Red crosses indicate lost dependencies in HDs and IgA deficiency.

Notably, enriched samples retained detectable levels of non-IgA-bound commensals. This analytical approach (33) was chosen, because it allows identification based on differential abundance, which is less sensitive to sample purity. We show that sIgA targets preferentially Firmicutes, Actinobacteria, and Proteobacteria, whereas Bacteroidetes are largely underrepresented compared to total microbiota composition. Only 1 of the 24 MGSs identified as preferred sIgA targets belongs to the Bacteroidetes phylum, despite its dominance in the human colon. Our results are consistent with previous mouse (12, 26) and human (26, 37–40) studies.

Although preferred IgA targets belong to the Firmicutes phylum, underrepresented bacteria in SIgAd patients are also Firmicutes, such as *Faecalibacterium*, a genus well known to exert anti-inflammatory effects on the gut mucosa (41) and which is notably depleted in IBDs (42, 43). Conversely, potentially proinflammatory Gammaproteobacteria and *Prevotella* (44) are overrepresented in SIgAd patients.

Overrepresented bacteria are more diverse than underrepresented bacteria. Three MGSs usually belonging to the oral flora (*V. parvula*, *S. sanguinis*, and *H. parainfluenzae*) are overrepresented in gut microbiomes of SIgAd patients. These bacteria are involved in biofilm formation and could exert inflammatory effects (45, 46). *V. parvula* has also been described as responsible for sepsis in an X-linked agammaglobulinemia patient (47). Finally, the genera usually described as pathogenic in patients (*Salmonella* and *Campylobacter*) were not found to be overrepresented.

Overall, we observed depletion of anti-inflammatory species, an expansion of proinflammatory species, and a lower digestive tract localization of constituents of the oral flora in IgAd patients. It was recently shown that ectopic localization of human salivary microbiota can elicit severe gut inflammation in susceptible host animals (48). It is therefore possible that ectopic oral microbiota could also exert a proinflammatory role in the context of SIgAd.

Table 1. Demographic and clinical cohort summary.

	HDs	SIgAd	P value*
Number of individuals	34	21	
Median age	32.9 (23–61)	36 (18–67)	0.1289
Sex ratio (F/M)	18:16	14:7	0.4708
IMC (index de masse corporelle)	21.9 (18.7–33.9)	22 (19.1–36)	0.3599
Ethnic origin [†]			0.1149
Caucasian	23 (68%)	18 (86%)	
North Africa	4 (11%)	3 (14%)	
Africa	1 (3%)	0 (0%)	
Middle eastern	4 (11%)	0 (0%)	
Asiatic	2 (5%)	0 (0%)	
Recurrent infections		9 (43%)	
Upper and lower respiratory tract		7 (33%)	
Intestinal		3 (14%)	
Vaginal		6 of 14 (43%)	
Antibiotics (>1 per year) [‡]		12 (57%)	
Autoimmune condition		11 (52%)	
Cytopenias		5 (24%)	
Systemic lupus erythematosus (SLE)		4 (19%)	
Thyroiditis		4 (19%)	
Celiac disease		2 (10%)	
Biermer anemia		1 (5%)	
Vitiligo		2 (10%)	
Type 1 diabetes		1 (5%)	
Ankylosing spondylitis		1 (5%)	
Intestinal symptoms (chronic diarrhea and/or chronic abdominal pain leading to digestive endoscopy)		9 (43%)	
Immunomodulatory therapy		3 (14%)	
Steroids [§]		3 (14%)	
Methotrexate		1 (5%)	
Hydroxychloroquine		3 (14%)	
Associated IgG4 subclass deficiency		2 (10%)	
Median IgG levels (mg/ml)	10.10 (6.7–15.2)	11.8 (7.14–18)	0.2475

*Continuous and discrete variables were assessed statistically with Mann-Whitney and χ^2 test for homogeneity, respectively. †All donors domesticated in France. ‡Four SIgAd patients having received antibiotics within 3 months from sampling were excluded for gut microbiota analysis but were included in the immunological phenotype analysis (compare Fig. 6). §Median dose of 10 mg/day.

Mechanisms underlying these findings are unknown, but one could speculate that sIgA, on the one hand, excludes (14, 49) and facilitates elimination of fast-growing pathobionts (50). On the other hand, sIgA could protect commensals by agglutination (51) and by localizing these bacteria in a favorable habitat like the mucus (fig. S8). Finally, IgA-mediated “intraluminal trapping” effects should prevent intimate bacterial proximity with the epithelial barrier and, therefore, host inflammation and associated negative effects on commensals.

In SIgAd patients, we show that the microbiota remains substantially bound by IgM. This observation, together with the recent characterization of dually coated (IgA⁺ IgM⁺) mucus-embedded bacteria

with increased richness compared to IgA-only-coated bacteria (52), suggests that IgM may compensate IgA deficiency. We show that microbial IgM binding is highly variable between patients. When focusing the analysis on commensals bound by sIgA in healthy subjects, or on differential genera between healthy controls and SIgAd patients, we noticed that IgM, like IgA, tends to preferentially bind *Clostridium*, *Bifidobacterium*, and *Faecalibacterium* (all Gram-positive bacteria). However, we show that IgM does not bind *Enterobacteriaceae*, nor *Prevotellaceae* families, which are overrepresented in SIgAd patients and involved in proinflammatory events (44). These data suggest that IgM is only partially efficient at controlling pathobionts,

accounting for the susceptibility to enteropathogens in SIgAd. Our data suggest that sIgA has the same positive impact at least on Firmicutes and Actinobacteria diversity in humans, whereas IgM would only favor the latter. Notably, the very narrow range of IgM binding to Firmicutes, and to some extent Proteobacteria, might have precluded identification of potential correlations between IgM binding and diversity in these phyla.

In an effort to determine whether Actinobacteria diversity would also be lost in the absence of IgM, we studied CVID gut microbiomes. We observed that Actinobacteria diversity is drastically decreased in CVID, an “IgM-deficient” model. Moreover, a similar trend is observed for Firmicutes. These results were confirmed in an independent CVID study. Jørgensen *et al.* (53) recently showed that CVID patients display dysbiotic gut microbiota with reduced α diversity, reduced abundance of Actinobacteria, and increased abundance of Gammaproteobacteria. It should be underlined that, although we took care to include CVID that did not receive antibiotics within 3 months before sampling, the analysis of CVID patients is potentially hampered by several confounders such as previous antibiotic courses and other treatments. It is, however, interesting to note that Actinobacteria diversity is preferentially decreased in two independent CVID studies, whereas other phyla are comparatively less affected in this IgM-deficient cohort, while, allegedly, confounding factors might have similarly affected all phyla. There is clinical relevance for this concept because it is well established that patients selectively lacking IgA rarely develop IBD, whereas this complication is more frequent and severe in those lacking both IgA and IgM (54).

The impact of IgA deficiency on bacterial symbiosis is further evidenced by the perturbation of bacterial networks. The presence in SIgAd patients of satellite bacteria (such as CAG 97, CAG 133, CAG 488, CAG 206, and CAG 328), in the absence of their previously described host (32), most probably reflects the establishment of novel dependency links. Such modifications underscore the role played by IgA well beyond its recognized neutralizing activity.

SIgAd has also profound systemic repercussions. The T_H17 bias that we observed is potentially connected to intestinal dysbiosis because Klemola *et al.* (55) have already shown the presence of activated T cells in gut mucosa of IgAd patients. As described by Perreau *et al.* (56), in CVID, $CD4^+PD-1^+$ cells are increased in SIgAd patients. Although LPS was not found to be elevated in SIgAd serum, increased sCD14 and PD-1 up-regulation could reflect T cell exhaustion induced by repeated bacterial translocation (57). Finally, and from a therapeutic perspective, a much larger cohort of patients would be needed to extract a potentially beneficial microbial signature associated with elevated IL-10 observed in some patients.

Together, we show that SIgAd in humans is associated with a mild intestinal dysbiosis, characterized by expansion of proinflammatory bacteria, depletion of anti-inflammatory commensals, and a perturbation in the “obligatory” bacterial network. Dysbiosis could be partly explained by the fact that IgA deficiency is not totally compensated by IgM secretion and by the loss of a nonredundant chaperone-like effect of IgA on microbial diversity.

MATERIALS AND METHODS

Study design

Patients and controls

We conducted a cross-sectional study of patients with IgA deficiency compared to healthy controls. Fresh stool and blood samples were collected simultaneously at a single time point in 21 patients with

SIgAd (table S1) and compared with 34 age- and sex-matched HDs (Table 1). We furthermore recruited seven CVID patients with IgA, IgG, and/or IgM deficiency, thus displaying a global antibody production defect. Patients were recruited from two French referral centers of clinical immunology (Department of Clinical Immunology in Saint Louis Hospital and Department of Internal Medicine in Pitié-Salpêtrière Hospital, Paris), where they were followed for clinical manifestations associated with antibody deficiencies. IgAd patient’s inclusion criteria were undetectable seric IgA levels (<0.07 mg/ml) in at least three previous samples in the past year. SIgAd is defined by serological means, namely, undetectable seric IgA titers (<0.07 mg/ml) with normal IgG levels. CVID patients are characterized by a marked decrease of seric IgG (at least 2 SD below the age-dependent mean) and a marked decrease in at least one of the isotypes IgM or IgA. For our study, we furthermore requested that the patients should be deficient in seric IgA (<0.07 mg/ml).

Exclusion criteria

Antibiotic therapy and laxative drugs use in the last 3 months before stool collection (inclusion for metagenomic analysis: 17 SIgAd patients, 7 CVID, and 34 HDs). Clinical and biological data were collected at inclusion time. Oral and written consent were obtained from patients before inclusion in the study.

Bioinformatical analysis

CAGs matrix construction

The projection of genes into CAGs was performed using a predefined list of 7381 CAGs (32). Every predefined CAG is a vector of genes ordered by increasing connectivity. For a bacterial genome, the most connected genes correspond to the marker genes present in all individuals carrying this organism (core genome). Starting with the gene frequency matrix, we projected the list of connected genes in each predefined CAG and extracted the corresponding frequency profile of the 50 most connected ones. Provided that at least 10% of marker genes are found, each frequency profile was used to compute the mean vector corresponding to the CAG frequency.

Differential CAGs identification

Genes from the gene profile matrix were used to identify those that were differentially abundant between the SIgAd patients and HD groups as described in (30). Briefly, Wilcoxon tests were used to compute the probabilities that gene frequency profiles did not differ between SIgAd patients and HD groups by chance alone. Benjamini and Hochberg multiple-test correction was applied to the P values. By performing a selection based on a significance threshold of $P < 0.01$, we identified 18,025 genes that were differentially abundant between the two groups. The same method and P value were applied to identify the differentially abundant genes between the IgA^+/IgA^- fractions in HDs. We identified 110,558 genes that were differentially abundant between the two groups. In a second step, the differentially abundant genes were projected into CAGs defined in the 3.9 million genes catalog. To validate a differential CAG, we used a threshold with a minimum of 50 differentially abundant genes per CAG (CAGs are kept only if they are equal to or exceed 50 connected genes) including at least 10% of marker genes. The frequency profile of the 50 most connected genes was used to compute the mean vector corresponding to the CAG frequency. Of the 18,025 differential genes between SIgAd patients and HDs, 8191 fell into 33 CAGs composed of 53 to 997 genes after the projection step (fig. S2B and data file S2). Thirty-one of the 33 CAGs are considered as MGS according to their gene size (≥ 700 genes). For the IgA^+ and IgA^- fraction comparisons, 80,415 of

110,558 differential genes fell into 119 CAGs of 50 to 3105 genes each. Thirty CAGs are overrepresented in the IgA⁺ fraction, and 89 are overrepresented in the IgA⁻ fraction. Twenty-four of the 30 IgA⁺ CAGs are considered MGS according to their gene size (fig. S5 and data file S3).

Wilcoxon tests were used to compute the probabilities that CAG frequency profiles did not differ between the two compared groups (SIgAd/HDs and IgA⁻/IgA⁺ fractions) by chance alone. Benjamini and Hochberg multiple-test correction was applied to the *P* values. The CAG taxonomical annotation was performed as previously described (58).

Dependency associations

Dependency associations between CAGs were defined as described previously (32). This analysis relies on the detection of CAGs that are systematically associated with other CAGs in *n* = 396 HDs. Briefly, dependencies between CAGs were based on their sample-wise overlapping detection. First, a Fisher exact test was used to identify statistically significant CAGs detection overlap. Second, the dependencies were validated only when the dependent CAGs were systematically observed with their associated host CAG. Thus, a dependent CAG, called satellite CAG, should never occur independently of the host CAG. Using these criteria, 886 dependencies were identified, most of which involved a small CAG as a satellite, corresponding to phage/bacteria or pan-genome/core-genome relationship. Moreover, 45 MGS-MGS dependency associations were detected, involving MGS as satellite and host microorganisms that may reflect bacterial symbiosis events. We have considered the 45 MGS-MGS dependency associations detected by Nielsen *et al.* (32) as a minimal obligatory network that should be retrieved in HDs, and we hypothesized that it could be disturbed in IgA deficiency. The presence of the 45 links was subsequently investigated in our cohort, and for each link, we have determined the frequency of its presence in both groups. On the basis of our HD frequency distributions, we have determined the 99% confidence interval according to the γ distribution law defining a threshold of frequency of 84%, below which the link was considered significantly decreased at the population level. The investigation of the 45-link presence-absence profiles in our cohort allowed us to distinguish four possible situations. For each link and each individual, if the MGS satellite is present in the absence of the host MGS, we consider the link as lost. If the MGS satellite is present in the presence of the host MGS, then we consider the link as confirmed. If the MGS host is present in the absence of the satellite MGS or if the two are absent, then the situation is not taken into account (no information about the link).

Statistical analysis

Log₂ ratio of IgM⁺/IgM⁻ bacterial abundances was performed at the lowest taxonomic identification level (genus or family) to analyze IgM⁺ relative binding. Only dominant taxa were taken into account, that is, taxa that are present in at least 50% of the patients. Zero was normalized in pairs and adjusted to the lowest abundance of all taxa in the paired samples.

Flow cytometry analysis was performed using FlowJo (9.3.2) TreeStar software and datamined with Funky Cells ToolBox software (version 0.1.2; www.FunkyCells.com). Statistical nonparametric tests were used whenever necessary: Mann-Whitney was used when comparing two groups, Kruskal-Wallis with multiple comparisons post-test of Dunn's was used when comparing three groups or more, Fisher's exact test was used for contingency, Wilcoxon paired rank test was used for paired analysis, and Spearman coefficient was used for correlations. R v3.2.1 and GraphPad Prism version 6 were used to perform statistical analysis.

SUPPLEMENTARY MATERIALS

www.sciencetranslationalmedicine.org/cgi/content/full/10/439/eaan1217/DC1
Materials and Methods

Fig. S1. Serum IgA and IgG concentration in IgAd patients.

Fig. S2. Global gut microbiota composition.

Fig. S3. Longitudinal stability of 24 IgA⁺ MGS abundances in three healthy subjects.

Fig. S4. Differential CAG abundance analysis between healthy subjects and IgAd patients.

Fig. S5. Differential CAG abundance analysis between IgA⁺ and IgA⁻ microbes.

Fig. S6. Gut microbiota IgA-binding patterns.

Fig. S7. Gut microbiota IgA and IgM binding in CVID patients with complete IgA deficiency.

Fig. S8. Model of the ecological impact of slgA binding on commensals.

Table S1. Individual clinical description of SIgAd patients.

Data file S1. MGS-MGS dependency network confirmation in IgAd patients (Excel file).

Data file S2. Thirty-three CAGs differentiating HDs and IgAd patients (Excel file).

Data file S3. One hundred nineteen CAGs differentiating gut microbiota in vivo bound by slgA or not in HDs (Excel file).

References (59–71)

REFERENCES AND NOTES

- M. J. Molloy, J. R. Grainger, N. Bouladoux, T. W. Hand, L. Y. Koo, S. Naik, M. Quinones, A. K. Dzutsev, J.-L. Gao, G. Trinchieri, P. M. Murphy, Y. Belkaid, Intraluminal containment of commensal outgrowth in the gut during infection-induced dysbiosis. *Cell Host Microbe* **14**, 318–328 (2013).
- S. Hapfelmeier, M. A. E. Lawson, E. Slack, J. K. Kirundi, M. Stoel, M. Heikenwalder, J. Cahenzli, Y. Velykoredko, M. L. Balmer, K. Endt, M. B. Geuking, R. Curtiss III, K. D. McCoy, A. J. Macpherson, Reversible microbial colonization of germ-free mice reveals the dynamics of IgA immune responses. *Science* **328**, 1705–1709 (2010).
- L. V. Hooper, A. J. Macpherson, Immune adaptations that maintain homeostasis with the intestinal microbiota. *Nat. Rev. Immunol.* **10**, 159–169 (2010).
- K. Suzuki, B. Meek, Y. Doi, M. Muramatsu, T. Chiba, T. Honjo, S. Fagarasan, Aberrant expansion of segmented filamentous bacteria in IgA-deficient gut. *Proc. Natl. Acad. Sci. U.S.A.* **101**, 1981–1986 (2004).
- S. Fagarasan, M. Muramatsu, K. Suzuki, H. Nagaoka, H. Hai, T. Honjo, Critical roles of activation-induced cytidine deaminase in the homeostasis of gut flora. *Science* **298**, 1424–1427 (2002).
- G. R. Harriman, M. Bogue, P. Rogers, M. Finegold, S. Pacheco, A. Bradley, Y. Zhang, I. N. Mbawuikie, Targeted deletion of the IgA constant region in mice leads to IgA deficiency with alterations in expression of other Ig isotypes. *J. Immunol.* **162**, 2521–2529 (1999).
- D. H. Reikvam, M. Derrien, R. Islam, A. Erofeev, V. Grcic, A. Sandvik, P. Gaustad, L. A. Meza-Zepeda, F. L. Jahnsen, H. Smidt, F.-E. Johansen, Epithelial-microbial crosstalk in polymeric Ig receptor deficient mice. *Eur. J. Immunol.* **42**, 2959–2970 (2012).
- O. L. C. Wijburg, T. K. Uren, K. Simpfendorfer, F.-E. Johansen, P. Brandtzaeg, R. A. Strugnell, Innate secretory antibodies protect against natural *Salmonella typhimurium* infection. *J. Exp. Med.* **203**, 21–26 (2006).
- N. Lycke, L. Erlandsson, L. Ekman, K. Schön, T. Leanderson, Lack of J chain inhibits the transport of gut IgA and abrogates the development of intestinal antitoxic protection. *J. Immunol.* **163**, 913–919 (1999).
- M. Wei, R. Shinkura, Y. Doi, M. Maruya, S. Fagarasan, T. Honjo, Mice carrying a knock-in mutation of *Aicda* resulting in a defect in somatic hypermutation have impaired gut homeostasis and compromised mucosal defense. *Nat. Immunol.* **12**, 264–270 (2011).
- S. Kawamoto, T. H. Tran, M. Maruya, K. Suzuki, Y. Doi, Y. Tsutsui, L. M. Kato, S. Fagarasan, The inhibitory receptor PD-1 regulates IgA selection and bacterial composition in the gut. *Science* **336**, 485–489 (2012).
- S. Kawamoto, M. Maruya, L. M. Kato, W. Suda, K. Atarashi, Y. Doi, Y. Tsutsui, H. Qin, K. Honda, T. Okada, M. Hattori, S. Fagarasan, Foxp3⁺ T cells regulate immunoglobulin A selection and facilitate diversification of bacterial species responsible for immune homeostasis. *Immunity* **41**, 152–165 (2014).
- J. J. Bunker, T. M. Flynn, J. C. Koval, D. G. Shaw, M. Meisel, B. D. McDonald, I. E. Ishizuka, A. L. Dent, P. C. Wilson, B. Jabri, D. A. Antonopoulos, A. Bendelac, Innate and adaptive humoral responses coat distinct commensal bacteria with immunoglobulin A. *Immunity* **43**, 541–553 (2015).
- C. R. Stokes, J. F. Sneath, M. W. Turner, Immune exclusion is a function of IgA. *Nature* **255**, 745–746 (1975).
- L. Yel, Selective IgA deficiency. *J. Clin. Immunol.* **30**, 10–16 (2010).
- N. Wang, L. Hammarström, IgA deficiency: What is new? *Curr. Opin. Allergy Clin. Immunol.* **12**, 602–608 (2012).
- G. H. Jorgensen, A. Gardulf, M. I. Sigurdsson, S. T. Sigurdardottir, I. Thorsteinsdottir, S. Gudmundsson, L. Hammarström, B. R. Ludviksson, Clinical symptoms in adults with selective IgA deficiency: A case-control study. *J. Clin. Immunol.* **33**, 742–747 (2013).
- S. Koskinen, Long-term follow-up of health in blood donors with primary selective IgA deficiency. *J. Clin. Immunol.* **16**, 165–170 (1996).

19. A. Aghamohammadi, T. Cheraghi, M. Gharagozlou, M. Movahedi, N. Rezaei, M. Yeganeh, M. Parvaneh, H. Abolhassani, Z. Pourpak, M. Moin, IgA deficiency: Correlation between clinical and immunological phenotypes. *J. Clin. Immunol.* **29**, 130–136 (2009).
20. J. F. Ludvigsson, M. Neovius, L. Hammarström, Association between IgA deficiency & other autoimmune conditions: A population-based matched cohort study. *J. Clin. Immunol.* **34**, 444–451 (2014).
21. L. Mellander, J. Björkander, B. Carlsson, L. Hanson, Secretory antibodies in IgA-deficient and immunosuppressed individuals. *J. Clin. Immunol.* **6**, 284–291 (1986).
22. P. Brandtzaeg, G. Karlsson, G. Hansson, B. Petruson, J. Björkander, L. A. Hanson, The clinical condition of IgA-deficient patients is related to the proportion of IgD- and IgM-producing cells in their nasal mucosa. *Clin. Exp. Immunol.* **67**, 626–636 (1987).
23. W. B. Chodirker, T. B. Tomasi Jr., Gamma-globulins: Quantitative relationships in human serum and nonvascular fluids. *Science* **142**, 1080–1081 (1963).
24. D. A. Peterson, N. P. McNulty, J. L. Guruge, J. I. Gordon, IgA response to symbiotic bacteria as a mediator of gut homeostasis. *Cell Host Microbe* **2**, 328–339 (2007).
25. T. C. Cullender, B. Chassaing, A. Janzon, K. A. Kumar, C. E. Muller, J. J. Werner, L. T. Angenent, M. E. Bell, A. G. Hay, D. A. Peterson, J. Walter, M. Vijay-Kumar, A. T. Gewirtz, R. E. Ley, Innate and adaptive immunity interact to quench microbiome flagellar motility in the gut. *Cell Host Microbe* **14**, 571–581 (2013).
26. N. W. Palm, M. R. de Zoete, T. W. Cullen, N. A. Barry, J. Stefanowski, L. Hao, P. H. Degnan, J. Hu, I. Peter, W. Zhang, E. Ruggiero, J. H. Cho, A. L. Goodman, R. A. Flavell, Immunoglobulin A coating identifies colitogenic bacteria in inflammatory bowel disease. *Cell* **158**, 1000–1010 (2014).
27. N. J. Mantis, N. Rol, B. Corthésy, Secretory IgA's complex roles in immunity and mucosal homeostasis in the gut. *Mucosal Immunol.* **4**, 603–611 (2011).
28. W. Al-Herz, A. Bousfiha, J.-L. Casanova, H. Chapel, M. E. Conley, C. Cunningham-Rundles, A. Etzioni, A. Fischer, J. L. Franco, R. S. Geha, L. Hammarström, S. Nonoyama, L. D. Notarangelo, H. D. Ochs, J. M. Puck, C. M. Roifman, R. Seger, M. L. K. Tang, Primary immunodeficiency diseases: An update on the classification from the International Union of Immunological Societies Expert Committee for Primary Immunodeficiency. *Front. Immunol.* **2**, 54 (2011).
29. K. Moor, J. Fadlallah, A. Toska, D. Sterlin, M. L. Balmer, A. J. Macpherson, G. Gorochov, M. Larsen, E. Slack, Analysis of bacterial-surface-specific antibodies in body fluids using bacterial flow cytometry. *Nat. Protoc.* **11**, 1531–1553 (2016).
30. J. Qin, R. Li, J. Raes, M. Arumugam, K. S. Burgdorf, C. Manichanh, T. Nielsen, N. Pons, F. Levenez, T. Yamada, D. R. Mende, J. Li, J. Xu, S. Li, D. Li, J. Cao, B. Wang, H. Liang, H. Zheng, Y. Xie, J. Tap, P. Lepage, M. Bertalan, J.-M. Batto, T. Hansen, D. Le Paslier, A. Linneberg, H. B. Nielsen, E. Pelletier, P. Renault, T. Sicheritz-Ponten, K. Turner, H. Zhu, C. Yu, S. Li, M. Jian, Y. Zhou, Y. Li, X. Zhang, S. Li, N. Qin, H. Yang, J. Wang, S. Brunak, J. Doré, F. Guarner, K. Kristiansen, O. Pedersen, J. Parkhill, J. Weissenbach; MetaHIT Consortium, P. Bork, S. D. Ehrlich, J. Wang, A human gut microbial gene catalogue established by metagenomic sequencing. *Nature* **464**, 59–65 (2010).
31. M. Arumugam, J. Raes, E. Pelletier, D. Le Paslier, T. Yamada, D. R. Mende, G. R. Fernandes, J. Tap, T. Bruls, J.-M. Batto, M. Bertalan, N. Borruel, F. Casellas, L. Fernandez, L. Gautier, T. Hansen, M. Hattori, T. Hayashi, M. Kleerebezem, K. Kurokawa, M. Leclerc, F. Levenez, C. Manichanh, H. B. Nielsen, T. Nielsen, N. Pons, J. Poulain, J. Qin, T. Sicheritz-Ponten, S. Tims, D. Torrents, E. Ugarte, E. G. Zoetendal, J. Wang, F. Guarner, O. Pedersen, W. M. de Vos, S. Brunak, J. Doré; MetaHIT Consortium, J. Weissenbach, S. D. Ehrlich, P. Bork, Enterotypes of the human gut microbiome. *Nature* **473**, 174–180 (2011).
32. H. B. Nielsen, M. Almeida, A. S. Juncker, S. Rasmussen, J. Li, S. Sunagawa, D. R. Plichta, L. Gautier, A. G. Pedersen, E. Le Chatelier, E. Pelletier, I. Bonde, T. Nielsen, C. Manichanh, M. Arumugam, J.-M. Batto, M. B. Q. dos Santos, N. Blom, N. Borruel, K. S. Burgdorf, F. Boumezeur, F. Casellas, J. Doré, P. Dworkowski, F. Guarner, T. Hansen, F. Hildebrand, R. S. Kaas, S. Kennedy, K. Kristiansen, J. R. Kultima, P. Léonard, F. Levenez, O. Lund, B. Mounen, D. Le Paslier, N. Pons, O. Pedersen, E. Prifti, J. Qin, J. Raes, S. Sørensen, J. Tap, S. Tims, D. W. Ussery, T. Yamada; MetaHIT Consortium, P. Renault, T. Sicheritz-Ponten, P. Bork, J. Wang, S. Brunak, S. D. Ehrlich, Identification and assembly of genomes and genetic elements in complex metagenomic samples without using reference genomes. *Nat. Biotechnol.* **32**, 822–828 (2014).
33. N. Qin, F. Yang, A. Li, E. Prifti, Y. Chen, L. Shao, J. Guo, E. Le Chatelier, J. Yao, L. Wu, J. Zhou, S. Ni, L. Liu, N. Pons, J. M. Batto, S. P. Kennedy, P. Leonard, C. Yuan, W. Ding, Y. Chen, X. Hu, B. Zheng, G. Qian, W. Xu, S. D. Ehrlich, S. Zheng, L. Li, Alterations of the human gut microbiome in liver cirrhosis. *Nature* **513**, 59–64 (2014).
34. F. Plaza Onate, J.-M. Batto, C. Juste, J. Fadlallah, C. Fougereux, D. Gouas, N. Pons, S. Kennedy, F. Levenez, J. Dore, S. D. Ehrlich, G. Gorochov, M. Larsen, Quality control of microbiota metagenomics by k-mer analysis. *BMC Genomics* **16**, 183 (2015).
35. P. Brandtzaeg, I. Fjellanger, S. T. Gjeruldsen, Immunoglobulin M: Local synthesis and selective secretion in patients with immunoglobulin A deficiency. *Science* **160**, 789–791 (1968).
36. U. Klein, R. Küppers, K. Rajewsky, Evidence for a large compartment of IgM-expressing memory B cells in humans. *Blood* **89**, 1288–1298 (1997).
37. A. L. Kau, J. D. Planer, J. Liu, S. Rao, T. Yatsunenko, I. Trehan, M. J. Manary, T.-C. Liu, T. S. Stappenbeck, K. M. Maleta, P. Ashorn, K. G. Dewey, E. R. Houpt, C.-S. Hsieh, J. I. Gordon, Functional characterization of IgA-targeted bacterial taxa from undernourished Malawian children that produce diet-dependent enteropathy. *Sci. Transl. Med.* **7**, 276ra24 (2015).
38. J. D. Planer, Y. Peng, A. L. Kau, L. V. Blanton, I. M. Ndao, P. I. Tarr, B. B. Warner, J. I. Gordon, Development of the gut microbiota and mucosal IgA responses in twins and gnotobiotic mice. *Nature* **534**, 263–266 (2016).
39. G. D'Auria, F. Peris-Bondia, M. Džunková, A. Mira, M. C. Collado, A. Latorre, A. Moya, Active and secreted IgA-coated bacterial fractions from the human gut reveal an under-represented microbiota core. *Sci. Rep.* **3**, 3515 (2013).
40. M. Džidic, T. Abrahamsson, A. Artacho, B. Björkstén, M. C. Collado, A. Mira, M. Jenmalm, Aberrant IgA responses to the gut microbiota during infancy precede asthma and allergy development. *J. Allergy Clin. Immunol.* **139**, 1017–1025.e14 (2017).
41. H. Sokol, B. Pigneur, L. Watterlot, O. Lakhdari, L. G. Bermúdez-Humarán, J.-J. Gratadoux, S. Blugeon, C. Bridonneau, J.-P. Furet, G. Corthier, C. Grangette, N. Vasquez, P. Pochart, G. Trugnan, G. Thomas, H. M. Blottière, J. Doré, P. Marteau, P. Seksik, P. Langella, *Faecalibacterium prausnitzii* is an anti-inflammatory commensal bacterium identified by gut microbiota analysis of Crohn disease patients. *Proc. Natl. Acad. Sci. U.S.A.* **105**, 16731–16736 (2008).
42. K. Machiels, M. Joossens, J. Sabino, V. De Preter, I. Arijis, V. Eeckhaut, V. Ballet, K. Claes, F. Van Immerseel, K. Verbeke, M. Ferrante, J. Verhaegen, P. Rutgeerts, S. Vermeire, A decrease of the butyrate-producing species *Roseburia hominis* and *Faecalibacterium prausnitzii* defines dysbiosis in patients with ulcerative colitis. *Gut* **63**, 1275–1283 (2014).
43. H. N. Sokol, P. Seksik, J. P. Furet, O. Firmesse, I. Nion-Larmurier, L. Beaugerie, J. Cosnes, G. Corthier, P. Marteau, J. Dore, Low counts of *Faecalibacterium prausnitzii* in colitis microbiota. *Inflamm. Bowel Dis.* **15**, 1183–1189 (2009).
44. E. Elinav, T. Strowig, A. L. Kau, J. Henao-Mejia, C. A. Thaiss, C. J. Booth, D. R. Peaper, J. Bertin, S. C. Eisenbarth, J. I. Gordon, R. A. Flavell, NLRP6 inflammasome regulates colonic microbial ecology and risk for colitis. *Cell* **145**, 745–757 (2011).
45. B. van den Bogert, M. Meijerink, E. G. Zoetendal, J. M. Wells, M. Kleerebezem, Immunomodulatory properties of *Streptococcus* and *Veillonella* isolates from the human small intestine microbiota. *PLOS ONE* **9**, e114277 (2014).
46. I. Mashima, F. Nakazawa, The influence of oral *Veillonella* species on biofilms formed by *Streptococcus* species. *Anaerobe* **28**, 54–61 (2014).
47. M. Strach, M. Siedlar, D. Kowalczyk, M. Zembala, T. Grodzicki, Sepsis caused by *Veillonella parvula* infection in a 17-year-old patient with X-linked agammaglobulinemia (Bruton's disease). *J. Clin. Microbiol.* **44**, 2655–2656 (2006).
48. K. Atarashi, W. Suda, C. Luo, T. Kawaguchi, I. Motoo, S. Narushima, Y. Kiguchi, K. Yasuma, E. Watanabe, T. Tanoue, C. A. Thaiss, M. Sato, K. Toyooka, H. S. Said, H. Yamagami, S. A. Rice, D. Gevers, R. C. Johnson, J. A. Segre, K. Chen, J. K. Kolls, E. Elinav, H. Morita, R. J. Xavier, M. Hattori, K. Honda, Ectopic colonization of oral bacteria in the intestine drives T_{H1} cell induction and inflammation. *Science* **358**, 359–365 (2017).
49. K. Moor, M. Diard, M. E. Sellin, B. Felmy, S. Y. Wotzka, A. Toska, E. Bakkeren, M. Arnoldini, F. Bansept, A. Dal Co, T. Völler, A. Minola, B. Fernandez-Rodriguez, G. Agatic, S. Barbieri, L. Piccoli, C. Casiraghi, D. Corti, A. Lanzavecchia, R. R. Regoes, C. Loverdo, R. Stocker, D. R. Brumley, W.-D. Hardt, E. Slack, High-avidity IgA protects the intestine by enchaining growing bacteria. *Nature* **544**, 498–502 (2017).
50. S. Okai, F. Usui, S. Yokota, Y. Hori-i, M. Hasegawa, T. Nakamura, M. Kurosawa, S. Okada, K. Yamamoto, E. Nishiyama, H. Mori, T. Yamada, K. Kurokawa, S. Matsumoto, M. Nanno, T. Naito, Y. Watanabe, T. Kato, E. Miyauchi, H. Ohno, R. Shinkura, High-affinity monoclonal IgA regulates gut microbiota and prevents colitis in mice. *Nat. Microbiol.* **1**, 16103 (2016).
51. A. Mathias, B. Corthésy, Recognition of gram-positive intestinal bacteria by hybridoma- and colostrum-derived secretory immunoglobulin A is mediated by carbohydrates. *J. Biol. Chem.* **286**, 17239–17247 (2011).
52. G. Magri, L. Comerma, M. Pybus, J. Sintes, D. Lligé, D. Segura-Garzon, S. Bascones, A. Yeste, E. K. Grasset, C. Gutzeit, M. Uzzan, M. Ramanujam, M. C. van Zelm, R. Albero-González, I. Vazquez, M. Iglesias, S. Serrano, L. Márquez, E. Mercade, S. Mehandru, A. Cerutti, Human secretory IgM emerges from plasma cells clonally related to gut memory B cells and targets highly diverse commensals. *Immunity* **47**, 118–134.e8 (2017).
53. S. F. Jørgensen, M. Trøseid, M. Kummén, J. A. Anmarkrud, A. E. Michelsen, L. T. Osnes, K. Holm, M. L. Høivik, A. Rashidi, C. P. Dahl, M. Vesterhus, B. Halvorsen, T. E. Mollnes, R. K. Berge, B. Moun, K. E. A. Lundin, B. Fevang, T. Ueland, T. H. Karlsen, P. Aukrust, J. R. Hov, Altered gut microbiota profile in common variable immunodeficiency associates with levels of lipopolysaccharide and markers of systemic immune activation. *Mucosal Immunol.* **9**, 1455–1465 (2016).
54. S. Agarwal, L. Mayer, Pathogenesis and treatment of gastrointestinal disease in antibody deficiency syndromes. *J. Allergy Clin. Immunol.* **124**, 658–664 (2009).
55. T. Klemola, E. Savilahti, A. Arato, T. Ormälä, J. Partanen, C. Eland, S. Koskimies, Immunohistochemical findings in jejunal specimens from patients with IgA deficiency. *Gut* **37**, 519–523 (1995).
56. M. Perreau, S. Viganò, F. Bellanger, C. Pellaton, G. Buss, D. Comte, T. Roger, C. Lacabaratz, P.-A. Bart, Y. Levy, G. Pantaleo, Exhaustion of bacteria-specific CD4 T cells and microbial translocation in common variable immunodeficiency disorders. *J. Exp. Med.* **211**, 2033–2045 (2014).

57. C. Chenevier-Gobeaux, D. Borderie, N. Weiss, T. Mallet-Coste, Y.-E. Claessens, Presepsin (sCD14-ST), an innate immune response marker in sepsis. *Clin. Chim. Acta* **450**, 97–103 (2015).
58. E. Le Chatelier, T. Nielsen, J. Qin, E. Prifti, F. Hildebrand, G. Falony, M. Almeida, M. Arumugam, J.-M. Batto, S. Kennedy, P. Leonard, J. Li, K. Burgdorf, N. Grarup, T. Jørgensen, I. Brandslund, H. B. Nielsen, A. S. Juncker, M. Bertalan, F. Levenez, N. Pons, S. Rasmussen, S. Sunagawa, J. Tap, S. Tims, E. G. Zoetendal, S. Brunak, K. Clément, J. Doré, M. Kleerebezem, K. Kristiansen, P. Renault, T. Sicheritz-Ponten, W. M. de Vos, J.-D. Zucker, J. Raes, T. Hansen; MetaHIT consortium, P. Bork, J. Wang, S. D. Ehrlich, O. Pedersen, E. Guedon, C. Delorme, S. Layec, G. Khaci, M. van de Guchte, G. Vandemeulebrouck, A. Jamet, R. Derwyn, N. Sanchez, E. Maguin, F. Haimet, Y. Winogradski, A. Cultrone, M. Leclerc, C. Juste, H. Blottière, E. Pelletier, D. LePaslier, F. Artiguenave, T. Bruls, J. Weissenbach, K. Turner, J. Parkhill, M. Antolin, C. Manichanh, F. Casellas, N. Boruel, E. Varela, A. Torrejon, F. Guarner, G. Denariáz, M. Derrien, J. E. van Hylckama Vlieg, P. Veiga, R. Oozeer, J. Knol, M. Rescigno, C. Brechot, C. M'Rini, A. Mérieux, T. Yamada, Richness of human gut microbiome correlates with metabolic markers. *Nature* **500**, 541–546 (2013).
59. D. M. Rissin, C. W. Kan, T. G. Campbell, S. C. Howes, D. R. Fournier, L. Song, T. Piech, P. P. Patel, L. Chang, A. J. Rivnak, E. P. Ferrell, J. D. Randall, G. K. Provuncher, D. R. Walt, D. C. Duffy, Single-molecule enzyme-linked immunosorbent assay detects serum proteins at subfemtomolar concentrations. *Nat. Biotechnol.* **28**, 595–599 (2010).
60. J.-P. Pais de Barros, T. Gautier, W. Sali, C. Adrie, H. Choubley, E. Charron, C. Lalande, N. Le Guern, V. Deckert, M. Monchi, J.-P. Quenot, L. Lagrost, Quantitative lipopolysaccharide analysis using HPLC/MS/MS and its combination with the limulus amoebocyte lysate assay. *J. Lipid Res.* **56**, 1363–1369 (2015).
61. M. Miyara, Y. Yoshioka, A. Kitoh, T. Shima, K. Wing, A. Niwa, C. Parizot, C. Tafin, T. Heike, D. Valeyre, A. Mathian, T. Nakahata, T. Yamaguchi, T. Nomura, M. Ono, Z. Amoura, G. Gorochoy, S. Sakaguchi, Functional delineation and differentiation dynamics of human CD4+ T cells expressing the FoxP3 transcription factor. *Immunity* **30**, 899–911 (2009).
62. M. Miyara, D. Chader, E. Sage, D. Sugiyama, H. Nishikawa, D. Bouvry, L. Claër, R. Hingorani, R. Balderas, J. Rohrer, N. Warner, A. Chapelier, D. Valeyre, R. Kannagi, S. Sakaguchi, Z. Amoura, G. Gorochoy, Sialyl Lewis x (CD15s) identifies highly differentiated and most suppressive FOXP3^{high} regulatory T cells in humans. *Proc. Natl. Acad. Sci. U.S.A.* **112**, 7225–7230 (2015).
63. C. Juste, D. P. Kreil, C. Beauvallet, A. Guillot, S. Vaca, C. Carapito, S. Mondot, P. Sykacek, H. Sokol, F. Blon, P. Lepercq, F. Levenez, B. Valot, W. Carré, V. Loux, N. Pons, O. David, B. Schaeffer, P. Lepage, P. Martin, V. Monnet, P. Seksik, L. Beaugerie, S. D. Ehrlich, J.-F. Gibrat, A. Van Dorsselaer, J. Doré, Bacterial protein signals are associated with Crohn's disease. *Gut* **63**, gutjnl-2012-303786 (2014).
64. J. J. Godon, E. Zumstein, P. Dabert, F. Habouzit, R. Moletta, Molecular microbial diversity of an anaerobic digester as determined by small-subunit rDNA sequence analysis. *Appl. Environ. Microbiol.* **63**, 2802–2813 (1997).
65. E. R. Mardis, The impact of next-generation sequencing technology on genetics. *Trends Genet.* **24**, 133–141 (2008).
66. B. Langmead, Aligning short sequencing reads with Bowtie. *Curr. Protoc. Bioinformatics* **32**, 11.7.1–11.7.14 (2010).
67. M.-A. Dillies, A. Rau, J. Aubert, C. Hennequet-Antier, M. Jeanmougin, N. Servant, C. Keime, G. Marot, D. Castel, J. Estelle, G. Guernec, B. Jagla, L. Jouneau, D. Laloë, C. Le Gall, B. Schaeffer, S. Le Crom, M. Guedj, J. Jaffrézic, A comprehensive evaluation of normalization methods for Illumina high-throughput RNA sequencing data analysis. *Brief. Bioinform.* **14**, 671–683 (2013).
68. K. H. Wilson, R. B. Blitchington, R. C. Greene, Amplification of bacterial 16S ribosomal DNA with polymerase chain reaction. *J. Clin. Microbiol.* **28**, 1942–1946 (1990).
69. J. G. Caporaso, J. Kuczynski, J. Stombaugh, K. Bittinger, F. D. Bushman, E. K. Costello, N. Fierer, A. G. Peña, J. K. Goodrich, J. I. Gordon, G. A. Huttley, S. T. Kelley, D. Knights, J. E. Koenig, R. E. Ley, C. A. Lozupone, D. McDonald, B. D. Muegge, M. Pirrung, J. Reeder, J. R. Sevinsky, P. J. Turnbaugh, W. A. Walters, J. Widmann, T. Yatsunenko, J. Zaneveld, R. Knight, QIIME allows analysis of high-throughput community sequencing data. *Nat. Methods* **7**, 335–336 (2010).
70. W. Li, A. Godzik, Cd-hit: A fast program for clustering and comparing large sets of protein or nucleotide sequences. *Bioinformatics* **22**, 1658–1659 (2006).
71. J. R. Cole, Q. Wang, E. Cardenas, J. Fish, B. Chai, R. J. Farris, A. S. Kulam-Syed-Mohideen, D. M. McGarrell, T. Marsh, G. M. Garrity, J. M. Tiedje, The Ribosomal Database Project: Improved alignments and new tools for rRNA analysis. *Nucleic Acids Res.* **37**, D141–D145 (2009).

Acknowledgments: We thank E. Slack and J.-M. Batto for discussions and advice, C. Fougeroux for assistance during lymphocyte and stool immunophenotyping initial setup, and J. R. Hov and S. F. Jørgensen for discussing their own unpublished microbiota diversity results in COVID patients. **Funding:** The study was financed by the following funding bodies: INSERM, Agence Nationale de la Recherche (ANR) (MetAntibody, ANR-14-CE14-0013), Fondation pour l'Aide à la Recherche sur la Sclérose En Plaques, and Université Pierre et Marie Curie Emergence (MycELIA). LPS measurements were supported by a French government grant managed by the French National Research Agency under the program "Investissements d'Avenir" with reference ANR-11 LABX-0021. **Author contributions:** J.F., M. Malphettes, L.G., D.B., A.M., M. Miyara, E.O., Z.A., and C.F. recruited the patients and collected the clinical data. J.F., D.S., D.G., C.J., and M.L. prepared the biospecimens (aliquoting and purification of live stool commensals) and cryopreserved them to generate biobank. J.F., D.S., C.P., C.J., and M.L. enriched the Ig-bound commensals. F.L., S.K., N.G., and N.P. generated the whole-genome metagenomic data. G.A., M.L., and P.L. generated the 16S data. J.F., C.P., D.G., D.S., and M.L. performed the flow cytometry analysis of patient lymphocytes and commensals. J.F., D.S., and K.D. measured the cytokine and sCD14 levels in donor serum. J.-P.P.d.B. measured the LPS levels in donor serum. J.F., H.E.K., M.A., E.L.C., and M.L. performed the data mining and biostatistical analysis. J.F., H.E.K., M.L., and G.G. designed the study, prepared the figures, and wrote the manuscript. S.D.E., J.D., P.L., and C.J. reviewed the manuscript. S.D.E., J.D., and C.J. provided support for the design of the study. **Competing interests:** The authors declare that they have no competing interests. **Data and materials availability:** The data presented in our study are available at <http://IgAdef.immulab.fr>.

Submitted 7 March 2017

Resubmitted 7 December 2017

Accepted 12 March 2018

Published 2 May 2018

10.1126/scitranslmed.aan1217

Citation: J. Fadlallah, H. El Kafsi, D. Sterlin, C. Juste, C. Parizot, K. Dorgham, G. Autaa, D. Gouas, M. Almeida, P. Lepage, N. Pons, E. Le Chatelier, F. Levenez, S. Kennedy, N. Galleron, J.-P. P. de Barros, M. Malphettes, L. Galicier, D. Boutboul, A. Mathian, M. Miyara, E. Oksenhendler, Z. Amoura, J. Doré, C. Fieschi, S. D. Ehrlich, M. Larsen, G. Gorochoy, Microbial ecology perturbation in human IgA deficiency. *Sci. Transl. Med.* **10**, eaan1217 (2018).

Microbial ecology perturbation in human IgA deficiency

Jehane Fadlallah, Hela El Kafsi, Delphine Sterlin, Catherine Juste, Christophe Parizot, Karim Dorgham, Gaëlle Autaa, Doriane Gouas, Mathieu Almeida, Patricia Lepage, Nicolas Pons, Emmanuelle Le Chatelier, Florence Levenez, Sean Kennedy, Nathalie Galleron, Jean-Paul Pais de Barros, Marion Malphettes, Lionel Galicier, David Boutboul, Alexis Mathian, Makoto Miyara, Eric Oksenhendler, Zahir Amoura, Joel Doré, Claire Fieschi, S. Dusko Ehrlich, Martin Larsen and Guy Gorochov

Sci Transl Med **10**, eaan1217.
DOI: 10.1126/scitranslmed.eaan1217

IgA leads the way in the gut

IgA is the most abundant mucosal antibody, and experiments with animal models suggest that it may enforce the gut barrier to prevent dangerous bacteria from damaging the host. However, humans deficient specifically in IgA often have only mild symptoms. Fadlallah *et al.* examined the fecal microbiomes of healthy individuals in comparison to those deficient in IgA. Overall bacterial diversity was comparable, but different genera were predominant in the patients. They investigated which bacteria were bound by different isotypes and concluded that IgM could partially compensate for the lack of IgA in patients, but not entirely. Their results suggest that, in humans, IgA is not solely responsible for controlling infections but does shape the microbiome.

ARTICLE TOOLS

<http://stm.sciencemag.org/content/10/439/eaan1217>

SUPPLEMENTARY MATERIALS

<http://stm.sciencemag.org/content/suppl/2018/04/30/10.439.eaan1217.DC1>

RELATED CONTENT

<http://stm.sciencemag.org/content/scitransmed/7/276/276ra24.full>
<http://stm.sciencemag.org/content/scitransmed/9/376/eaaf9655.full>
<http://stm.sciencemag.org/content/scitransmed/8/343/343ra81.full>

REFERENCES

This article cites 71 articles, 22 of which you can access for free
<http://stm.sciencemag.org/content/10/439/eaan1217#BIBL>

PERMISSIONS

<http://www.sciencemag.org/help/reprints-and-permissions>

Use of this article is subject to the [Terms of Service](#)